Remote Sensing of Environment 200 (2017) 183–205

Contents lists available at ScienceDirect

Remote Sensing of Environment

journal homepage: www.elsevier.com/locate/rse

A novel strategy for wetland area extraction using multispectral MODIS data

Sangeeta Bansal, Deeksha Katyal, J.K. Garg*

University School of Environment Management, Guru Gobind Singh Indraprastha University, Delhi 110078, India

ARTICLE INFO

Keywords:
Wetlands
MODIS
Data mining
Separability analysis
Wetland Model Index

ABSTRACT

MODIS (Moderate Resolution Imaging Spectro-radiometer) is an imaging sensor onboard Terra/Aqua platform which provides information in 36 spectral bands. Spectral mixing of features due to high data dimensionality and high inter-band correlations constitutes the biggest challenge in the analysis of MODIS data. In view of this, present study attempts to develop a novel strategy involving Principal Component Analysis (PCA), Band to Band Correlation (BTBC) analysis, Stepwise Discriminant Analysis (SDA), and separability analysis to reduce the data dimensionality for extracting reliable and maximum information for wetland areal extent using coarse resolution MODIS (1 km) data. The PCA explains variability in data and removes data redundant information; BTBC analysis eradicates the high correlated bands providing best bands suitable for wetland mapping; SDA evaluates the discriminatory power of different MODIS bands to discriminate the wetlands from other class types. Further, Normalized Difference Vegetation Index (NDVI) and Wetland Model Index (WMI) were also incorporated into the study to improve the classification accuracy. Finally, separability analysis was conducted to optimize the selected MODIS bands and indices.

Results of rigorous data mining reveal that out of 24 input layers of MODIS (1 km) data (22 optical MODIS bands, NDVI and WMI), only 4 input layers (WMI, NDVI, MODIS bands – NIR band 2 and SWIR band 6) are best suited for delineation and mapping of wetlands. This study also corroborates the usage of WMI, a newly developed index with combination of visible and short wavelength infra red (SWIR) MODIS bands, as the most optimal input layer to separate wetlands from the other land use class types (barren land, agricultural land, rivers/canals/streams, forest, wasteland/gullied or riverine land). It was observed that the magnitude of mapped wetland areal extent using MODIS (1 km) data varied from 105,053 ha in 2010–2011 to 111,479 ha in 2011–2012 accounting for 0.44% (2010–2011)–0.46% (2011–2012) of the total geographical area of Uttar Pradesh, India. Seasonally, monsoon season displayed maximum wetland area with overall accuracy of 92% whereas summer season exhibited minimum wetland area with overall accuracies varying from 85 to 87% during both the sampling years. The output of the present research work will not only facilitate to improve the wetland area estimates but also provide an important input for climate change predictions in wetlands over large areas.

1. Introduction

Being the largest natural emitter of greenhouse gases predominantly methane, wetlands have been considered as one of the most evocative area in climate change studies. The areal extent of wetlands particularly lentic water systems (lakes/ponds/reservoirs/waterlogged and marshy areas) exhibits wide temporal fluctuations which have an immense impact on oxygenic conditions in these wetlands affecting the rates of various microbial mediated processes such as methane production and oxidation, soil respiration and ecosystem respiration. Therefore, precise spatio-temporal estimation of areal extent (water spread/volume and number) of wetlands is paramount to monitor the various microbial mediated processes in wetlands. Remote sensing (RS) and Geographic Information System (GIS) have emerged as a powerful and an indispensable source of multi-temporal and spatial measures of land surface. Many studies have been carried out to map and assess the spatio-temporal changes of wetlands (Garg et al., 1998; Alphan and Yilmaz, 2005; SAC, 2011; Chen et al., 2014; Garg, 2015) deploying different analytical techniques to extract reliable information about wetland's areal extent. There is no single best approach available for wetland delineation and classification using remote sensing data and the choice of the best technique to map wetland areas is highly objective specific. Accordingly, in the present study, MODIS (1 km) data has been used for estimation of wetland areas (lakes/ponds/reservoirs/waterlogged and marshy areas) at regional level due to its large area coverage and high temporal resolution.

* Corresponding author.
E-mail address: jkgarg@ipu.ac.in (J.K. Garg).

http://dx.doi.org/10.1016/j.rse.2017.07.034
Received 24 December 2016; Received in revised form 21 July 2017; Accepted 30 July 2017

MODIS sensor onboard AQUA and TERRA satellites of NASA's Earth Observation System (EOS), provides multi-temporal and multispectral coarse resolution satellite data in 36 narrow spectral bands all through visible, near infra red (NIR), middle infra red (MIR), short wavelength infra red (SWIR) and thermal bands of the electromagnetic spectrum with 250 m (1 and 2 bands), 500 m (3 to 7 bands) and 1 km (remaining bands) spatial resolutions. Depending upon whether it is on Terra or Aqua platform, it provides data in ascending (10:30 am) and descending (1:30 pm) modes. It scans earth ± 55° from nadir and acquire along and across track observations to enhance the knowledge for understanding the various dynamic phenomena of the earth surface (http://modis.gsfc. nasa.gov/about/).

MODIS data provides an excellent opportunity to carry out research on global environmental issues. A number of standard MODIS data products (such as evapotranspiration, land cover, net photosynthesis and primary productivity, land surface temperature and emissivity etc.) have been utilized by scientific community for various research purposes. Nonetheless, the digital analysis of coarse resolution multispectral MODIS data, including pre-processing, is quite different from the conventional broadband analysis. The major problems associated with the analysis of MODIS data involve inter-band correlation and high data dimensionality leading to the spectral mixing of the features. Thus, it is imperative that the volume and dimensionality of the data should be reduced to few bands containing relevant information so that traditional classification methods can be applied for information extraction. In view of this, three data mining techniques including Principal Component Analysis (PCA), Band to Band Correlation (BTBC) analysis and Stepwise Discriminant Analysis (SDA) have been applied in the present study to extract optimal MODIS bands from MODIS Terra products of 1 km spatial resolution to reduce the data dimensionality.

PCA, a multivariate statistical technique, has been effectively employed in the field of remote sensing for image data transformation and compression in change detection studies. Chakraborty (2009) performed PCA to detect the forest changes in Barak Basin of northeastern India covering the states of Assam, Manipur, Mizoram, Nagaland and Tripura using MODIS Terra (Vegetation Index) products of 250 m resolution for each year from 2000 to 2006. Likewise, Hillger and Clark (2002) analyzed the infrared bands of MODIS to identify the suitable bands for detecting the volcanic ash using Principal Component Analysis for Popocatepetl volcano near Mexico City and Cleveland volcano in the Aleutian Islands. It was found that all the 36 bands of MODIS provide good flexibility for ash detection but MODIS bands 28–32 were found to be most suitable for detecting airborne volcanic ash. In the present study, PCA is used to select the optimal MODIS wavebands for wetland delineation and mapping over larger areas.

SDA technique has also been applied for feature extraction and change detection on multi/hyperspectral datasets in a number of studies. Galvao et al. (2005) used SDA to select the best variables among surface reflectance values, ratios of reflectance and spectral indices potentially sensitive to changes in chlorophyll content, leaf water and lignin-cellulose for discriminating sugarcane varieties. It was observed that SDA could classify four sugarcane varieties with similar reflectance with a classification accuracy of 88%. Miettinen (2007) performed SDA to determine the most effective band combinations to distinguish between burnt and unburnt areas for each land cover type using MODIS data in Borneo for investigating fire induced spectral changes in surface reflectance from different land cover types. Analysis of results showed that indices or combinations of indices developed by using B1, B2 and B7 bands of MODIS were observed to be potentially effective for burnt-area detection in majority of the areas. Similarly, SDA has also been adopted in the current study to assess the discriminatory power of various bands of MODIS (1 km) data in separating wetlands from other land cover types.

BTBC analysis as a standalone technique is not very effective and is preferably utilized in conjunction with other data mining techniques. Miglani et al. (2008) carried out BTBC analysis in conjunction with PCA on hyperspectral data acquired from Hyperion sensor onboard EO-1 of NASA to extract the optimal bands for agricultural applications. According to this study, out of total 242 bands, 196 bands were found to be useful on the basis of preliminary data analysis. Further, out of 196 bands only 20 bands were selected on the basis of maximum contribution of these bands to first five principal components and the band combinations with least inter-band correlations. In the present investigation, BTBC analysis has been carried out in conjunction with PCA and SDA to extract the least correlated MODIS bands with distinctive and relevant information for wetland classification.

A new technique of separability analysis has been developed and applied to optimize MODIS bands extracted via data mining techniques of PCA, BTBC analysis and SDA in combination with indices including NDVI and WMI to map wetlands. NDVI and WMI were incorporated into the study to further improve the classification accuracy. Spectral indices, mathematical combinations of spectral bands available in satellite data, have been developed for maximizing the sensitivity of certain land surface properties and minimizing the effects due to sensor viewing geometry, solar illumination, atmospheric distortions, topography, and instrument noise etc. to allow the consistent spatial and temporal comparisons (Liang, 2004; Ray et al., 2007).

Several spectral indices are widely used for prediction and monitoring of several land surface processes in wetlands. NDVI is one of the most significant indexes deployed in wetland mapping and classification due to its sensitivity to vegetated and non-vegetated areas within and outside the wetlands. For instance, NDVI has been successfully utilized in mapping wetland areas in West Songnen Plain, Northeast China (Dong et al., 2014). In India, NDVI has also been considered an important input in generating state-wise wetland maps (SAC, 2011). This study also recommends a new-fangled index for wetland delineation and mapping known as Wetland Model Index (WMI). WMI, developed through random arithmetical combinations of green (band 4) and SWIR (band 6) bands of MODIS (1 km) data, can discriminate the wetlands from other land features due its sensitivity to water spread and water content of vegetation and soil in wetlands.

Eventually, considering the major drawback of spectral mixing of wetlands with other land cover types i.e., barren land (BL), agricultural land (AL), rivers/canals/streams (RCS), forest (FR), wasteland/gullied or riverine land (WL) due to high data dimensionality and inter-band correlations of MODIS (1 km) datasets, present research has been planned with the main objectives of i) investigating the potential of PCA, SDA and BTBC analysis in conjunction with separability analysis for maximizing wetland information extraction with a minimum number of MODIS bands/indices, ii) exploring the efficacy of newly developed MODIS WMI in discriminating wetlands from other land cover types, and iii) developing a suitable strategy for wetland area extraction over large areas using coarse resolution MODIS (1 km) datasets.

2. Data and methods

2.1. Study area

Study was carried out for the state of Uttar Pradesh (UP) which lies between 23° 45′ to 30° 30′ N latitudes and 77° to 84° 45′ E longitudes and occupies substantial part of high wetland density tropical zone of India (Fig. 1).

The state shows large physical variability and broadly comprises three physiographic units including i) the Sub-Himalayan Zone of Terai Bhabar and the foothills of Siwaliks, ii) the Alluvial Gangetic Plain covering nearly two-third of UP built by Ganga and its tributaries, and iii) the Peninsular Region which represents the southernmost part of the UP. The eastern part of this region comprises the Vindhyan mountains whereas rocky highland plateau, composed of Bundelkhand granite and gneiss, lies in the western part (Jha, 2007).

As UP is a state of great physiographical diversity, it supports large

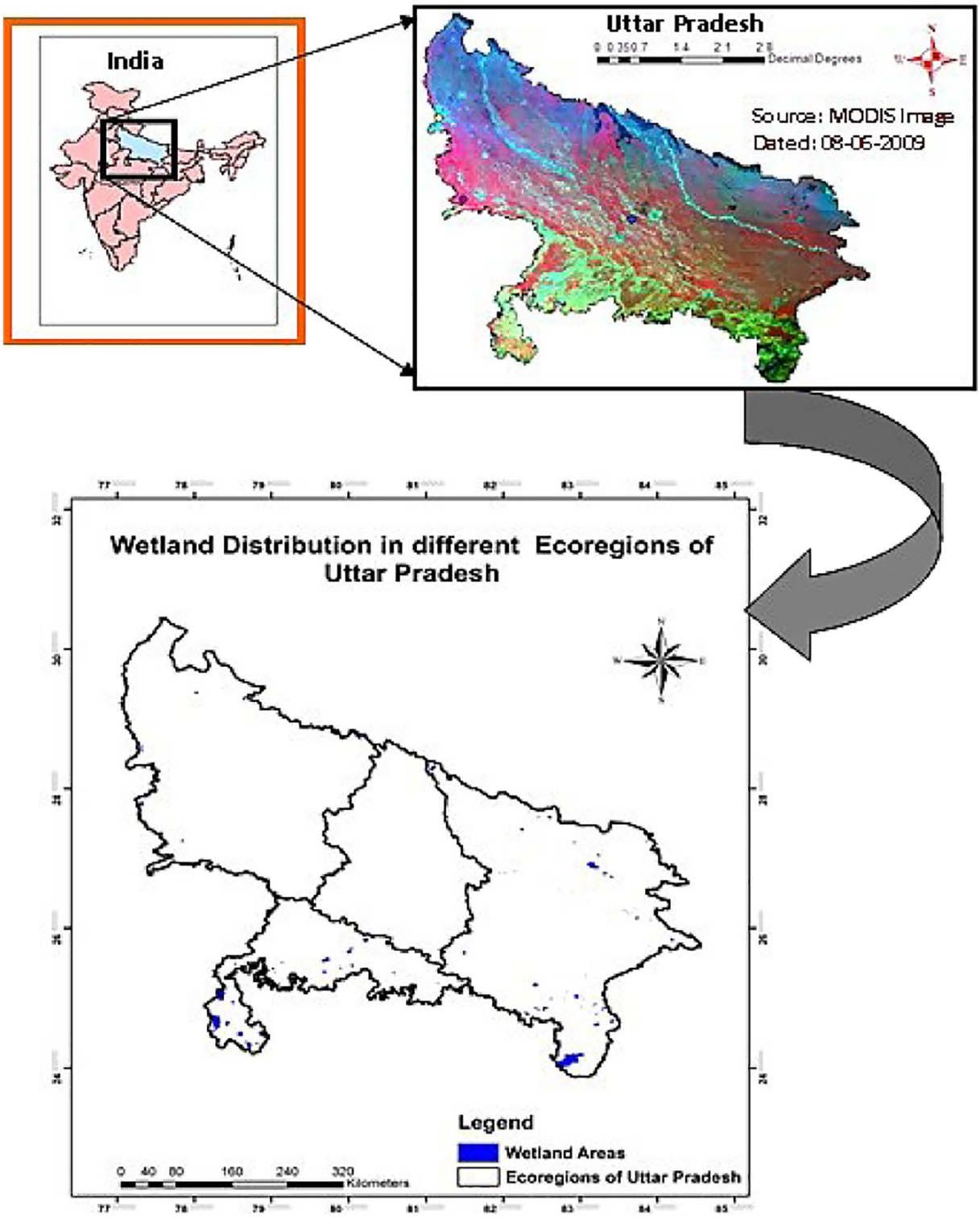

Fig. 1. Location map of study area showing wetland distribution in Uttar Pradesh.

and diverse wetland classes. The Ganga and Yamuna are the two major rivers of Uttar Pradesh. Large numbers of lakes, ponds, tanks, reservoirs, dams, canals, marshy areas are distributed all over the state. According to the SAC (2011) report, total wetland area in Uttar Pradesh is about 1,242,530 ha including rivers which is around 5.16% of its geographical area of 24, 092, 800 ha.

2.2. Satellite data used

Cloud free multi-date raw MODIS datasets with spatial resolution of 1 km for the year 2010–2011 and 2011–2012 covering entire state of Uttar Pradesh were browsed and downloaded from LADSWEB website and processed. Details of MODIS data used are summarized in Table 1.

Table 1
Details of MODIS (1 km) data used.

Date of data acquisition	MODIS product code
24-10-2010 (monsoon-2010)	MODO21KM.A2010297.0510.005.2010297133904.hdf
09-02-2011 (winter-2011)	MODO21KM.A2011040.0535.005.2011040145747.hdf
05-06-2011 (summer-2011)	MODO21KM.A2011156.0510.005.2011156183651.hdf
02-10-2011 (monsoon-2011)	MODO21KM.A2011275.0515.005.2011275131145.hdf
11-10-2011 (monsoon-2011)	MODO21KM.A2011284.0510.005.2011284173504.hdf
26-02-2012 (winter-2012)	MODO21KM.A2012057.0545.005.2012057132415.hdf
02-05-2012 (summer-2012)	MODO21KM.A2012123.0535.005.2012123133041.hdf

2.3. Pre-processing of MODIS (1 km) data

Raw MODIS (1 km) datasets were processed using image processing software ENVI Version 4.7 and ERDAS 14.0. Raw image of the required date was geocorrected with reference to Survey of India state toposheet/map of Uttar Pradesh at 1:1,000,000 scale. The bowtie correction was applied to restore the original geometry of the image. Georectified first 22 MODIS bands (Table A1) were then stacked together to extract area of interest (UP) for further processing.

2.4. Data dimensionality reduction

In the present study, data mining techniques including PCA, SDA, and BTBC analysis were applied to reduce the data dimensionality of MODIS (1 km) datasets to extract optimal bands.

PCA reduces or removes the redundancy present in multi/hyperspectral data by compressing the information content of original data set into a new data set containing few uncorrelated variables which are known as principal components. It rotates the original data axes in such a manner so that the brightness values on the original axes are redistributed on to new set of axes which are orthogonal to each other (Thenkabail et al., 2004; Fung and Ledrew, 1987). In any Principal Component Rotation, the first component (PC1) accounts for the maximum percentage of the variance of the original data or image, and succeeding components (PC2, PC3 and so on) contain less amount of variance. Thus, transformation of the raw remote sensor data using PCA can result in new principal component images that may be more interpretable than the original data (Singh and Harrison, 1985). In the present study, input bands (MODIS wavebands with 1 km calibrated radiances) having maximum and pertinent information were selected on the basis of loading factors or contribution of various input bands to the first and second principal components obtained after this orthogonal transformation of the data set using I/P software ENVI Version 4.7.

BTBC analysis was also carried out using I/P software ENVI Version 4.7. The correlation of each input band with the remaining bands was estimated by developing a correlation matrix with all possible combinations of input bands. The correlation values (R) were calculated either below or above the diagonal of the matrix, as values on either side were transpose of one another. The correlation values (R) were then converted to R^2 to nullify the effect of negative sign and facilitate better interpretation of correlation results (Thenkabail et al., 2004; Miglani, 2009).

Stepwise Discriminant Analysis (SDA) is another data mining technique which aims to select the most optimal bands out of the group of multi/hyper spectral bands using multivariate separability statistics such as Wilks' Lambda, F-value etc. (Thenkabail, 2002). In the present work, SDA was conducted by locating the region of interest (ROIs) for all the classes under consideration i.e., wetland, BL, AL, RCS, FR and WL deploying I/P software ENVI Version 4.7. These ROIs were utilized to estimate respective spectral values using MS-Excel software for Windows. The SDA was performed using these spectral values in SPSS 16.0 statistical software for Windows. The first three spectral bands with least to lower Wilk's Lambda values generated via SDA for each season during both the sampling years were selected for further analysis. This is because more the number of spectral bands added to the image dataset, SDA model loses it stability due to increasing correlation and decreasing discriminatory power between the bands.

2.5. Development of spectral indices

In the present investigation, NDVI (Rouse et al., 1973) and a new spectral index, WMI, have been developed via random mathematical combinations of MODIS optical bands of 1 km spatial resolution using ERDAS Imagine Modeler tool (ERDAS Imagine 14.0). Since NDVI provides a measure of vegetation density in an image, it was used to locate vegetated and non-vegetated areas within and outside the wetlands (Fig. 2). Similarly, WMI can clearly delineate the wetlands boundaries from other land cover types as the SWIR band 6 (1.628–1.653 μm) which WMI uses is a strong water absorption band and is sensitive to variations in water spread as well as water content of vegetation and soil in wetlands. Accordingly, WMI was used to discern wetland and non-wetland areas because the water bodies exhibit negative WMI values in comparison to other features and display darker tone in WMI imagery (Fig. 2). The mathematical formulae of NDVI and WMI are as follows:

$$\mathrm{NDVI} = (\mathbf{R_{NIR}} - \mathbf{R_{RED}})/(\mathbf{R_{NIR}} + \mathbf{R_{RED}})$$

$$\mathrm{WMI} = (\mathbf{R_{SWIR}} - \mathbf{R_{GREEN}})/(\mathbf{R_{SWIR}} + \mathbf{R_{GREEN}})$$

where $\mathbf{R_{NIR}}$, $\mathbf{R_{RED}}$, $\mathbf{R_{GREEN}}$, and $\mathbf{R_{SWIR}}$ are the 1 km calibrated spectral reflectance/radiance values in NIR (band 2), red (band 1), green (band 4) and SWIR (band 6) bands respectively. The values of both the indices varied from −1 to 1. Positive NDVI and WMI values indicated vegetated areas and non-wetland areas whereas negative NDVI and WMI values represented non-vegetated and wetlands areas respectively. Thus, both the indices exhibit negative values for wetlands.

2.6. Separability analysis

Separability analysis was carried out to assess separability power of optimal MODIS bands selected through PCA, SDA and BTBC analysis, NDVI, and WMI to segregate wetlands from other land class types i.e., BL, AL, RCS, FR and WL. Therefore, best MODIS bands sorted out from three data mining techniques were stacked with NDVI and WMI into a single image file to identify the ROIs for all the classes under consideration to calculate respective spectral values.

Based on these spectral values, mean radiance values were calculated for each class in all the input layers (bands/indices). Further, this measure of central tendency (mean radiance value of wetlands) was plotted against mean radiance values of each other class type (BL, AL, RCS, FR and WL) for each input layer to generate mean radiance plots known as wetland spectral curves. To analyze the separability power of each band/index in each wetland spectral curve, ± 0.1 of mean radiance value of wetland for each layer has been considered a scale factor to determine the lower and upper limit of each input layer to separate wetlands from each other class type. If for two classes (wetland versus BL/wetland versus AL/wetland versus RCS/wetland versus FR/

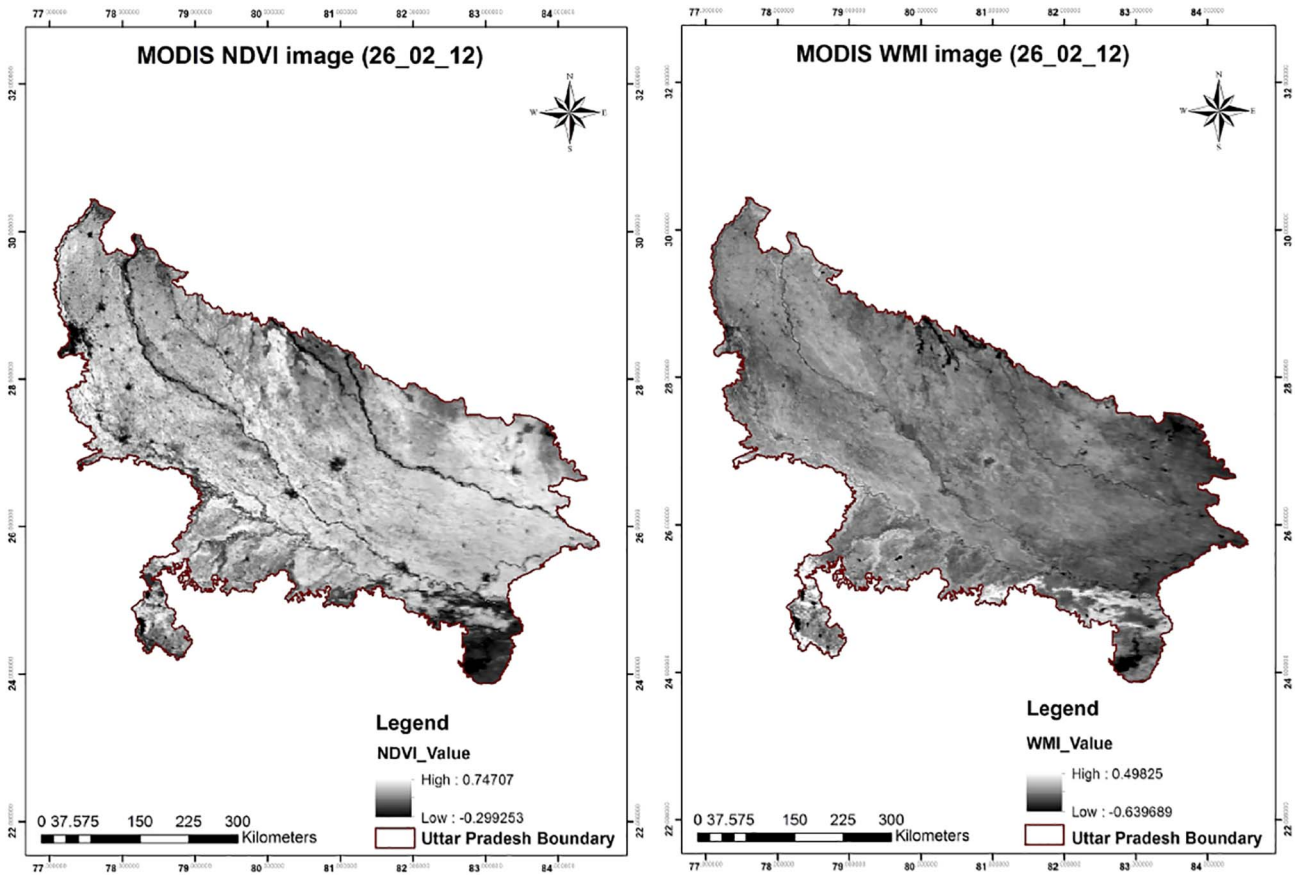

Fig. 2. Spectral indices used for wetland area extraction.
(*NDVI and WMI were estimated for all the MODIS (1 km) datasets mentioned in Table 1).

wetland versus WL), mean radiance value of any input band/index lies within the desired limits, it is considered that the band/index is not discriminating the classes significantly. Wetland spectral curves were then used to generate wetland separability tables to compute the wetland separability factor for each input layer. Finally, the input layers with high values of wetland separability factor were utilized for further analysis.

2.7. Wetland mapping

The optimal MODIS bands (bands 2 and 6) and indices (NDVI and WMI) were stacked together to generate season-wise classified final MODIS images for wetland area estimation during 2010–2011 and 2011–2012 using unsupervised classification and onscreen visual interpretation. Unsupervised classification and on-screen interpretation are two traditional methods of image classification. In unsupervised classification, clustering algorithms such as K-Means and Iterative Self-Organizing Data (Isodata) algorithms are used to determine the spectral classes on the basis of spectral signatures/numerical information of the data as this technique is based on the fact that similar classes cluster in a feature space. In unsupervised classification, to carry out clustering, initial cluster (class) means are computed for all evenly distributed clusters in the data and then pixels are assigned the clusters using a minimum distance technique iteratively. Each iteration recalculates cluster means and reclassifies pixels in relation to new means. All pixels are classified to the nearest clusters unless a distance threshold is achieved and some of pixels remained unclassified as they do not meet the desired criteria. This procedure is continued until the maximum number of iterations is reached. Spectral classes are then grouped by the analyst by matching each class with class to which it most probably belongs. Although no *priori* knowledge (training sets of known classes) is required, the analyst attempts a posteriori (after the fact) to assign appropriate groups to these spectral class and for this analyst should understand the spectral characteristics of the terrain well enough to label certain clusters as representing information classes (Jensen, 1996). So, there may be some discrepancy in classification results owing to less familiarity of the analyst with the study area. Therefore, accuracy of this method can be improved by examining the images visually on the basis of characteristics such as tone, shape, size, pattern, texture, shadow, location, association and height in high resolution maps/photographs/images (Joseph, 2005). Accordingly, combination of unsupervised classification (Isodata) and visual interpretation was deployed to map wetlands in the present study. Onscreen visual interpretation of MODIS (1 km) data was done in consonance with National Remote Sensing Centre (NRSC) land use – land cover (LULC) maps and medium resolution Advanced Wide Field Sensor (AWiFS) imagery onboard Resourcesat − 2 for October–November 2010 (Tables A2 and A3).

To discriminate wetlands from other classes including BL, AL, RCS, FR and WL (Table A4), these land cover types were merged into a single non-wetland class. Also, as MODIS is a coarse resolution data, separation between open water and aquatic vegetation (emergent) is very difficult due to spectral mixing of wetland features. Consequently, only two land cover types i.e., wetland and non-wetland areas were extracted to detect the seasonal changes in wetland areal extent during 2010–2011 and 2011–2012 employing multi-temporal MODIS (1 km) data (Fig. 3).

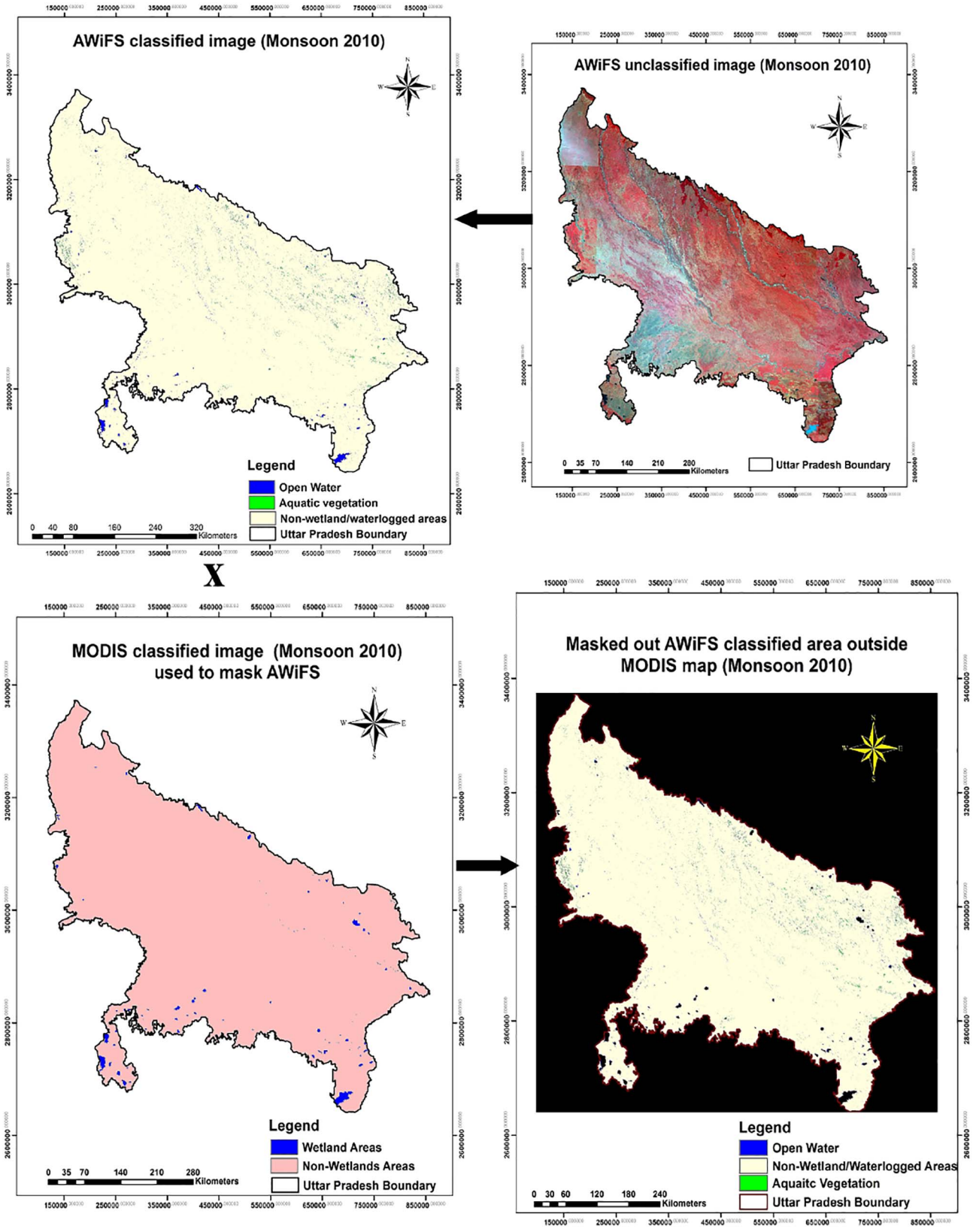

Fig. 3. Steps involved in WAF-FRI method to extract wetland area fraction from a finer resolution AWiFS imagery.

Table 2
Accuracy assessment of wetland area mapped using AWiFS (56 m) data.

Wetland feature	Producer accuracy (%)	User accuracy (%)
Open water	90.00	84.00
Aquatic vegetation	80.00	100.00
Non-wetland areas	97.00	91.00
Overall accuracy (%) = 89.00		
Kappa coefficient = 0.835		

Further, mixed pixels in coarse resolution MODIS (1 km) data can reduce the accuracy of classification as only a fraction of a coarse pixel falls under a particular land cover type (Thenkabail et al., 2007). So, in studies where coarse resolution datasets are used, sub-pixel areas which represent the actual areas should be preferred over full pixel areas. Considering this, in the present study, sub-pixel wetland area was computed for MODIS (1 km) datasets using medium resolution AWiFS (56 m) data to minimize the errors in MODIS (1 km) wetland area estimates. This method of using finer-resolution data to calculate sub-pixel areas of the coarser resolution imagery is known as WAF-FRI

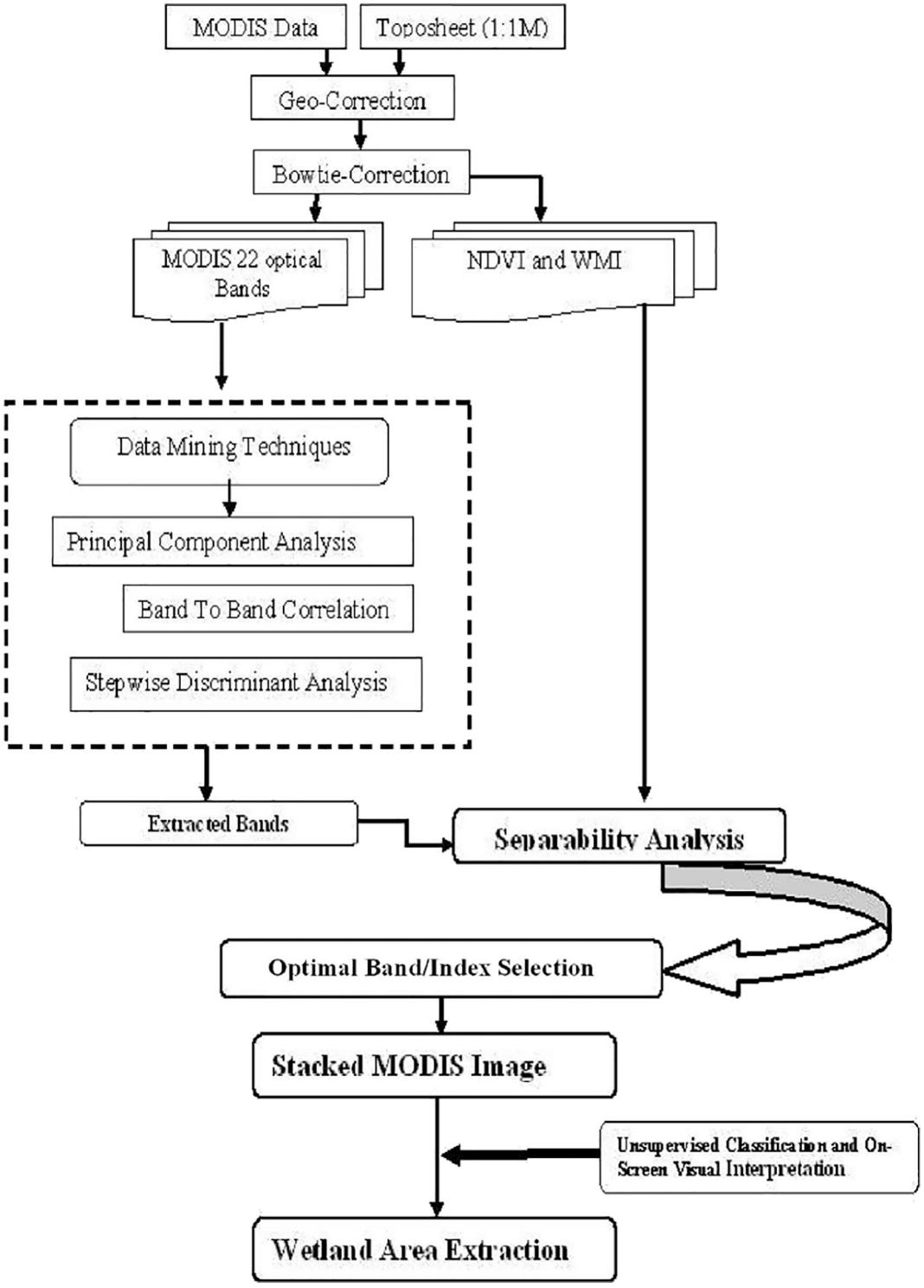

Fig. 4. Schematic of methodology used.

Table 3
Results of Principal Component Analysis (PCA).

Season	Input bands with first five highest loading factors in first 2 PCs							
	2010–2011				2011–2012			
	PC1		PC2		PC1		PC2	
Monsoon	Band 5	0.0981	Band 15	0.8547	Band 17	0.4403	Band 15	0.7587
	Band 2	0.0864	Band 13	0.3162	Band 16	0.4400	Band 13	0.5211
	Band 6	0.0770	Band 2	0.0430	Band 18	0.4397	Band 2	0.0433
	Band 19	0.0682	Band 5	0.0324	Band 14	0.4373	Band 19	0.0315
	Band 8	0.0669	Band 19	0.0309	Band 13	0.3496	Band 5	0.0273
% variability explained	89.87		7.66		87.07		9.46	
Winter	Band 5	0.0979	Band 18	0.2506	Band 22	0.0471	Band 6	0.5948
	Band 2	0.0974	Band 17	0.2504	Band 14	0.0362	Band 12	0.4369
	Band 19	0.0856	Band 7	0.0263	Band 1	0.0327	Band 9	0.1890
	Band 6	0.0665	Band 1	0.0118	Band 8	0.0308	Band 15	0.1194
	Band 21	0.0580	Band 6	0.0080	Band 19	0.0269	Band 1	0.1062
% variability explained	84.60		8.07		88.07		8.83	
Summer	Band 5	0.1305	Band 12	0.9216	Band 5	0.1123	–	–
	Band 6	0.1249	Band 11	0.3172	Band 6	0.1081	–	–
	Band 2	0.1134	Band 8	0.0064	Band 2	0.0923	–	–
	Band 7	0.0936	Band 22	− 0.0006	Band 7	0.0807	–	–
	Band 19	0.0852	Band 2	− 0.0013	Band 19	0.0775	–	–
% variability explained	89.09		7.42		99.31		–	

(Wetland Area Fraction-Finer Resolution Imagery) method. Similar method of IAF-HRI (Irrigated Area Fraction-High Resolution Imagery) was earlier illustrated by Thenkabail et al. (2007) to calculate sub-pixel irrigated areas. Following are the steps involved in WAF-FRI method for estimating sub-pixel wetlands areas for MODIS (1 km) data (Fig. 3):

A. Downloading of AWiFS (56 m) data from Bhuvan-Gateway to Indian Earth Observation (bhuvan.nrsc.gov.in/data/download/index.php) for nearly the same time period i.e., October–November 2010 (Monsoon 2010) and analyzing following the same analytical techniques as used in case of MODIS (1 km) datasets to extract three classes including open water, aquatic vegetation and non-wetland areas (Fig. 3) with overall accuracy and Kappa coefficient of 89% and 0.835 respectively (Table 2).
B. Estimating total AWiFS (56 m) wetland area of Uttar Pradesh by summing up AWiFS area calculated under open water and aquatic vegetation.
C. Overlaying classified AWiFS (Monsoon 2010) imagery on MODIS (1 km) class area map of monsoon 2010 to mask out the wetland area of AWiFS (Monsoon 2010) imagery that was outside the MODIS (1 km) classified image of monsoon 2010 for calculating WAF for AWiFS (Monsoon 2010) imagery (Fig. 3).
D. Computing sub-pixel wetland areas for all MODIS (1 km) datasets by multiplying MODIS (1 km) full pixel area estimated for each dataset with the WAF estimated using finer resolution AWiFS (56 m) imagery (Monsoon 2010) to get actual areas.

2.8. Accuracy assessment

Accuracy assessment of each MODIS (1 km) as well as AWiFS (56 m) dataset was accomplished using ERDAS Imagine 14.0. A sample of 30 random points for each class (60 points for MODIS and 90 for AWiFS) was generated for each MODIS (1 km) as well as AWiFS (56 m) dataset on Google Earth imagery (http://earth.google.com) to produce confusion matrix to provide the user's, producer's and overall accuracies for each method. K static was also utilized to assess the reliability of all the applied classification methods. Schema of methodology used in the present research is shown in Fig. 4.

3. Results

3.1. Principal Component Analysis (PCA)

PCA was applied on the stacked MODIS image of 1 km spatial resolution consisting of 22 optical bands. It was observed that for each season in both the sampling years, first 2 principal components (PC's) contain maximum information content explaining $\geq 90\%$ of the variability for each dataset (Table 3). The subsequent PC's merely accounted for $\leq 10\%$ of total variability explained, and thus were not taken into consideration.

It is also evident from the Fig. 5, as the PC's increase in number, noise in the data gets enhanced in the form of stripping/speckle, making them unsuitable for further analysis. Resultantly, the wavebands contributing to first 2 PC's for each data set have been selected to carry out present research work. Further, the importance of first five input bands in each PC was assessed by their respective loading factors to top 2 PC's as shown in Table 3.

PCA results showed that for monsoon season in both the years, PC1 and PC2 were loaded with visible (VIS; bands-8, 13, 14, 15) and NIR (bands-5, 2, 16, 17, 18, 19) regions of the electromagnetic spectrum (EMS). Similarly, in winter 2010–2011, both 1st and 2nd PC were mainly dominated by NIR (bands-5, 2, 17, 18, 19) region with two SWIR bands including bands 6 and 7 whereas in winter 2011–2012, both the first two PC's were heavily loaded by VIS region (bands-1, 8, 9, 12, 14, 15). On the other hand, NIR (bands-2, 5, 19) and SWIR (bands 6 and 7) regions of the EMS were found to be dominating in summer season during both the years i.e., 2010–2011 and 2011–2012. Finally, 22 wavebands got reduced to two PC wavebands indicating the overall dominance of NIR bands (2, 5 and 19) for all seasons during the entire study period.

3.2. Band to Band Correlation (BTBC) analysis

The main underpin of this method is that the input band pairs with least interband correlations (R^2) contain maximum and distinctive information (Thenkabail et al., 2004; Miglani, 2009). On the contrary, band pairs with redundant information exhibit very high correlation

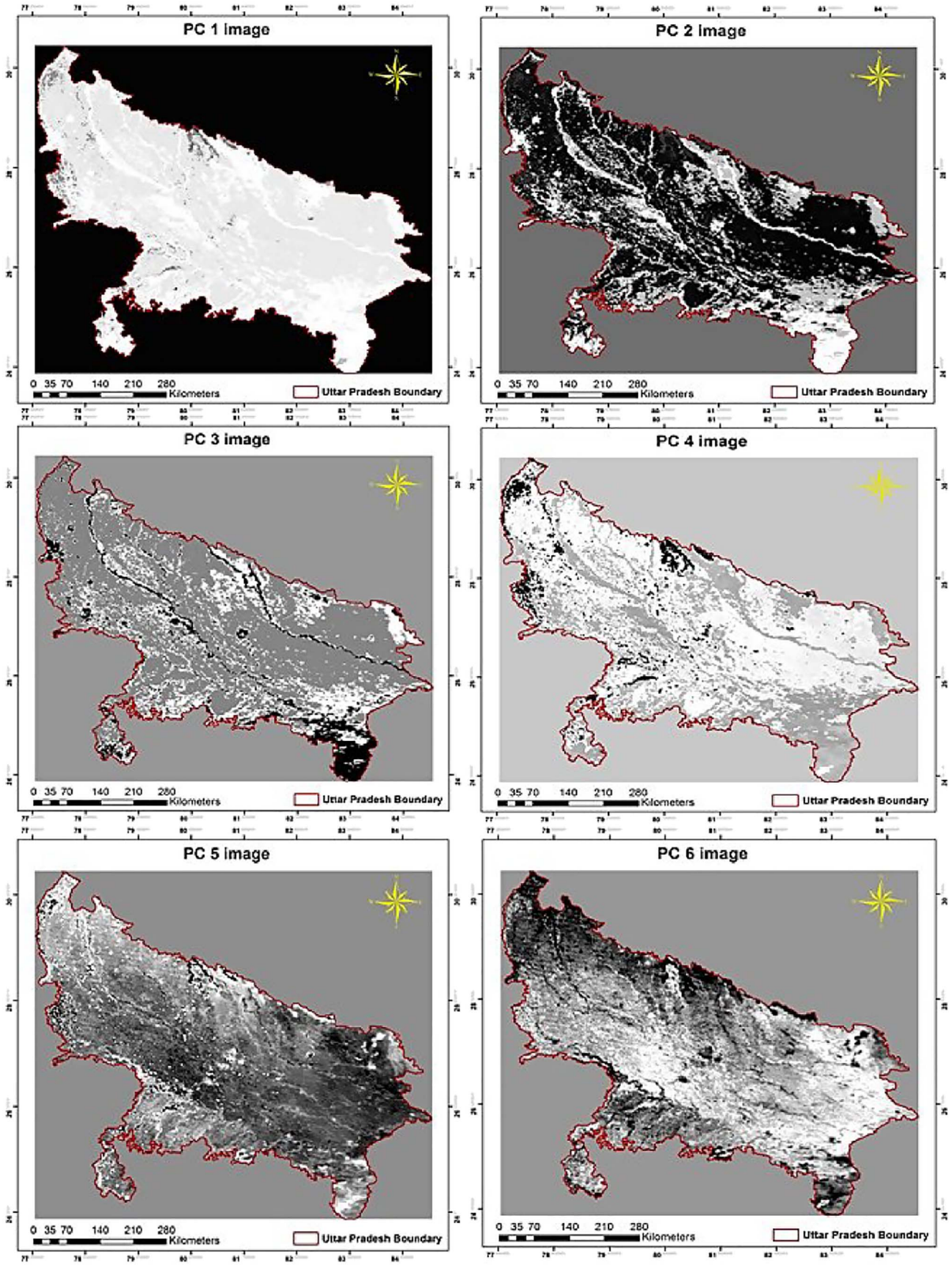

Fig. 5. Principal component images (PC1-PC6) extracted using MODIS (1 km) data for 26-02-2012.
(*Similar principal component images were generated for all the MODIS (1 km) datasets used in the study).

Table 4
Band to Band Correlation (BTBC) analysis to select least correlated band pairs.

Season	First two input bands pairs with least correlation (R^2)					
	2010–2011			2011–2012		
	Band pairs		R^2	Band pairs		R^2
Monsoon	Band 5	Band 22	0.0046	Band 15	Band 22	0.0008
	Band 2	Band 22	0.0085	Band 13	Band 22	0.0903
Winter	Band 21	Band 15	0.00005	Band 15	Band 20	0.0000
	Band 15	Band 19	0.00006	Band 17	Band 15	0.0001
Summer	Band 5	Band 11	0.00001	Band 12	Band 22	0.2830
	Band 3	Band 11	0.00002	Band 11	Band 22	0.4574

(R^2) values (Thenkabail et al., 2004; Miglani, 2009). In this method, a 22 × 22 band correlation matrix was generated which correlates each input waveband with every other waveband. The correlation values (R^2) were calculated for 22 band pairs for each season for each year. Table 4 highlights the first two band pairs extracted via BTBC analysis for every season during both the years. These band pairs were least correlated with each other and contain distinctive and relevant information. It can also be inferred that most of the least correlated bands lie in the VIS and NIR regions of the EMS. Season-wise R^2 values for other band pairs extracted from BTBC analysis for both the years are summarized in Tables A5, A6 and A7.

3.3. Stepwise Discriminant Analysis (SDA)

SDA was carried out to assess the discriminatory power of multispectral MODIS (1 km) data to separate the wetlands from other different land cover types including BL, AL, RCS, FR and WL. In this technique, at each step, variable or input band that minimizes the overall Wilks' Lambda and maximizes the overall F value is entered to sort out the bands having highest discriminatory power. The Wilks' Lambda ranges from 0 to 1. Zero value of Wilks' Lambda represents the perfect separability between the bands. On the other hand, bands contain repetitive or similar information if the value of Wilks' Lambda is equal to one. Thus, bands with lowest Wilks' Lambda value and highest F value represent highest discriminatory power. Accordingly, first three input bands for every season during each year were selected as these bands show maximum information and discriminatory power with least

Table 5
Seasonal Wilk's Lambda and F values for selecting appropriate bands possessing high discriminatory powers.

Wilk's Lambda and F values											
2010–2011						2011–2012					
Input waveband	Wilk's Lambda	F value	df1	df2	Sig.	Input waveband	Wilk's Lambda	F value	df1	df2	Sig.
Monsoon											
Band 2	0.204	3506.071	5	4498	0.000	Band 5	0.277	2560.691	5	4895	0.000
Band 19	0.215	3288.000	5	4498	0.000	Band 19	0.279	2531.492	5	4895	0.000
Band 21	0.268	2453.402	5	4498	0.000	Band 2	0.281	2503.473	5	4895	0.000
Winter											
Band 13	0.252	2064.3	5	3486	0.00	Band 20	0.258	2078.6	5	3605	0.000
Band 15	0.280	1797.0	5	3486	0.00	Band 21	0.258	2071.3	5	3605	0.000
Band 4	0.304	1597.2	5	3486	0.00	Band 19	0.276	1888.1	5	3605	0.000
Summer											
Band 4	0.322	1558.803	5	3703	0.000	Band 4	0.4376	964.509	5	3752	0.000
Band 10	0.356	1337.974	5	3703	0.000	Band 1	0.4422	946.523	5	3752	0.000
Band 3	0.366	1282.768	5	3703	0.000	Band 3	0.4977	757.405	5	3752	0.000

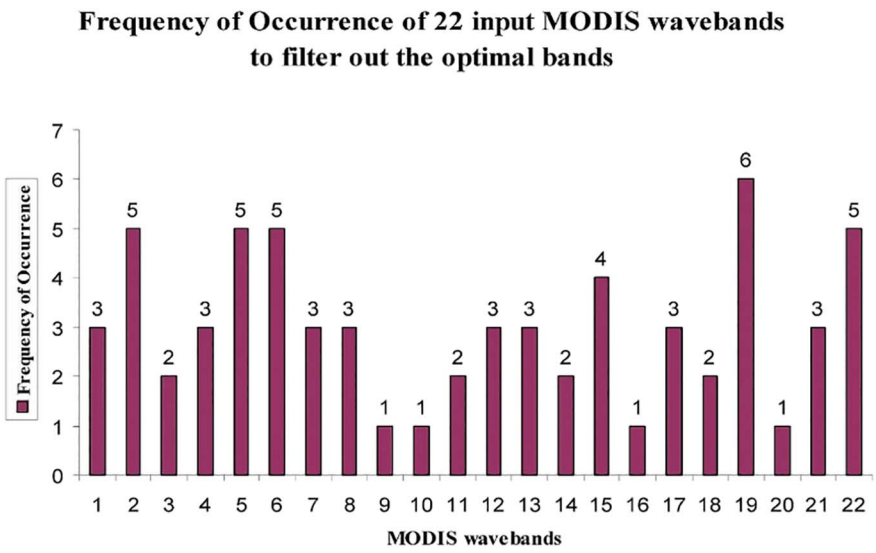

Fig. 6. Frequency occurrence plot used to select the optimal MODIS bands following the data mining process.

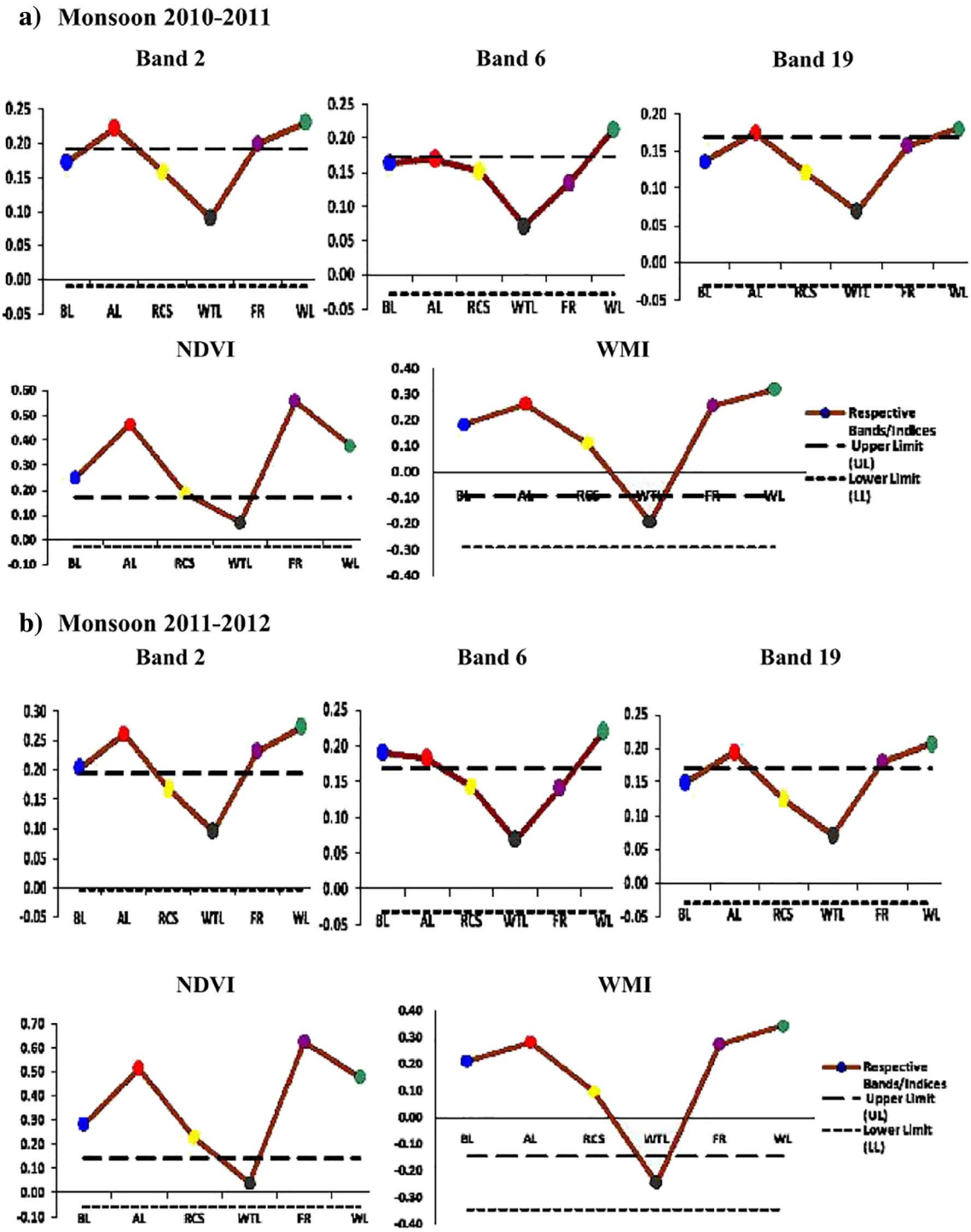

Fig. 7. Wetland (WTL) spectral curves for monsoon season.
*X-axis represents class types considered in the present research work.
*Y-axis represents mean reflectance/radiance for each class in each respective band/index.

to lower Wilk's Lambda values (Table 5). Season-wise Wilks' Lambda and F values estimated for other input bands during both the years have been provided in Tables A8, A9 and A10.

3.4. Separability analysis results

The optimal MODIS bands extracted using PCA, BTBC analysis and SDA were summed up to determine their frequency of occurrence (FOC) in all six MODIS (1 km) datasets used in analysis i.e., three season (monsoon, winter and summer) datasets for each sampling year. Frequency occurrence plot (Fig. 6) divulges that band 19 (NIR band) was the most frequently occurring waveband with maximum FOC of 6 whereas bands including 2, 5, 6, and 22 displayed the second highest FOC of 5. Resultantly, the dimensionality of data set was reduced from 22 MODIS bands to 5 MODIS bands (2, 5, 6, 19 and 22). Further, the suitability of selected MODIS bands and Indices (NDVI and WMI) for wetland delineation and mapping was optimized through separability analysis.

Separability analysis was conducted on the composite image containing 5 input layers i.e., 3 optimal MODIS bands (2, 6 and 19)

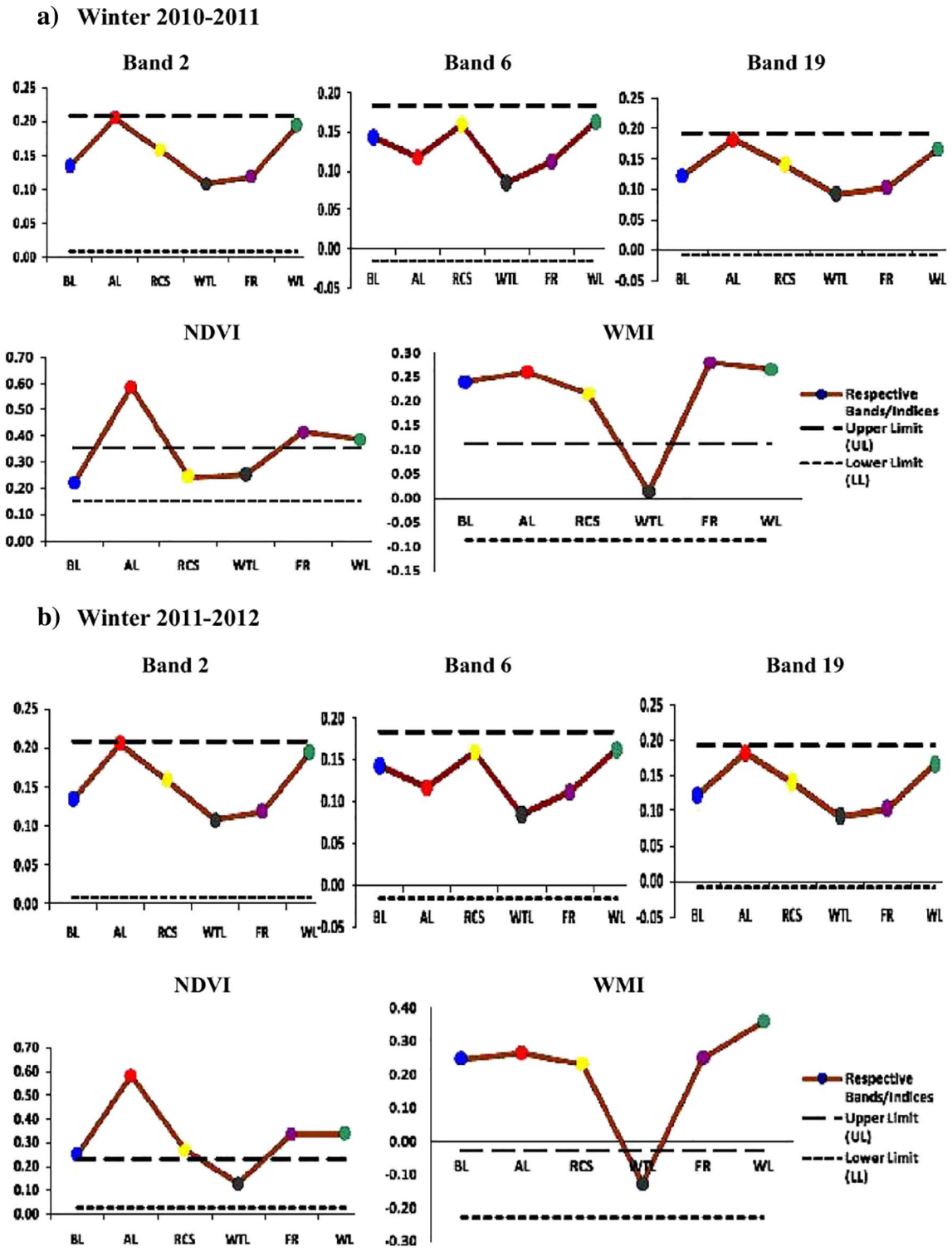

Fig. 8. Wetland (WTL) spectral curves for winter season.
*X-axis represents class types considered in the present research work.
*Y-axis represents mean reflectance/radiance for each class in each respective band/index.

extracted from PCA, SDA and BTBC analysis, NDVI, and WMI to determine the importance of each band/index in separation of wetlands from other land cover types. MODIS wavebands 2, 6, and 19 were found to be optimal for separability analysis because of high FOC values of 6 (band 19) and 5 (bands 2 and 6). Though MODIS wavebands 5 and 22 also showed second highest FOC of 5 (Fig. 6) but were discarded in separability analysis due to band stripping.

As discussed in the section on methodology, ± 0.1 of mean radiance value of wetland for each band/index has been considered to estimate the lower and upper limit for generating wetland spectral curves and wetland separability tables for the selected bands and indices. For instance, in monsoon 2010–2011, the mean radiance value for wetlands in MODIS band 2 is 0.0906. Hence, upper limit and lower limits are 0.1906 and − 0.0094 respectively. Wetland spectral curves (Figs. 7, 8, and 9) and separability tables (Tables 6, 7 and 8) showed the discrimination capability of each band and index to delineate wetlands

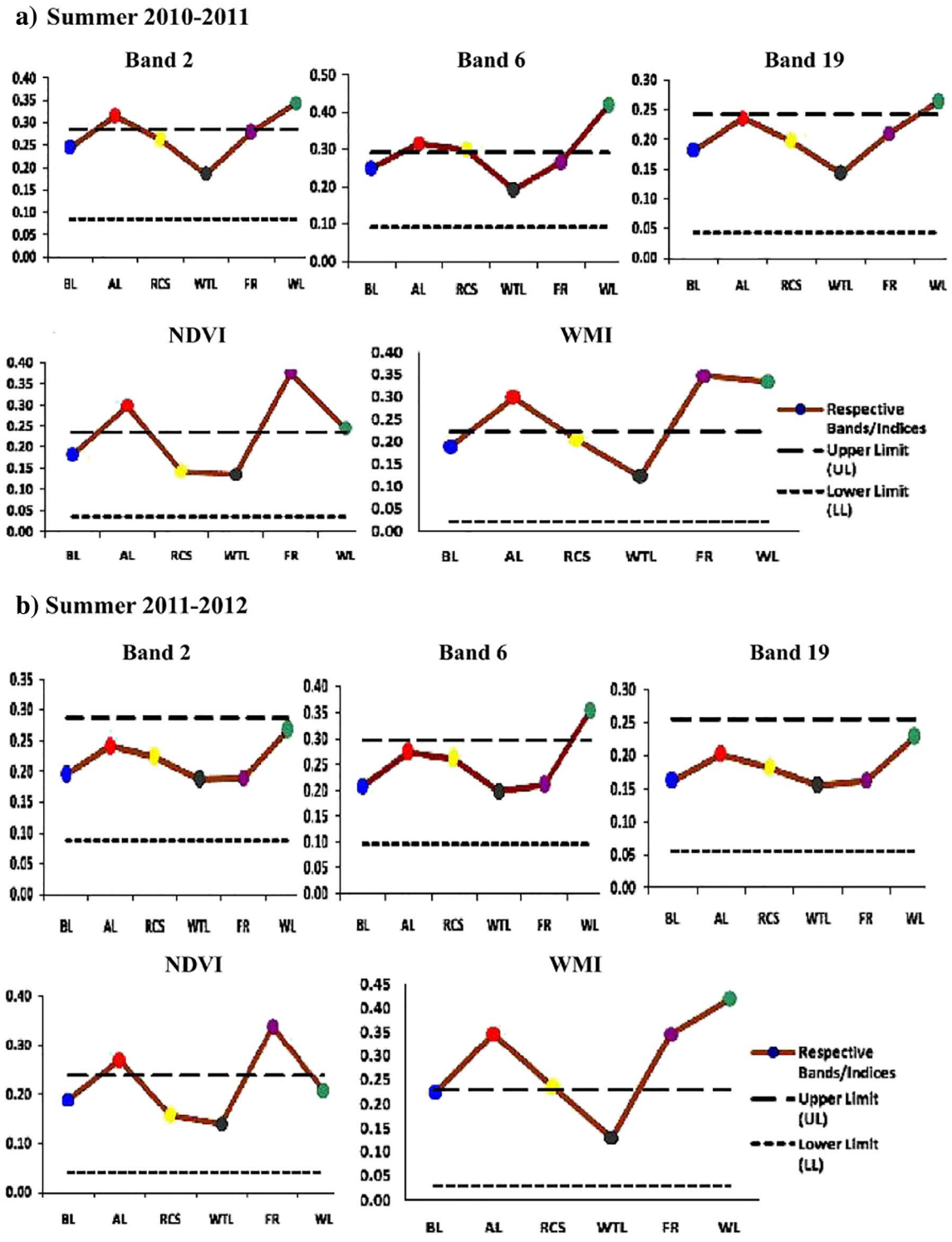

Fig. 9. Wetland (WTL) spectral curves for summer season.
*X-axis represents class types considered in the present research work.
*Y-axis represents mean reflectance/radiance for each class in each respective band/index.

Table 6
Wetland spectral separability for monsoon season generated using MODIS (1 km) data.

Wetland separability	Bands/indices				
	B2	B6	B19	NDVI	WMI
Monsoon - 2010–2011					
Wetland from BL	No	Yes	No	Yes	Yes
Wetland from AL	Yes	Yes	Yes	Yes	Yes
Wetland from RCS	No	No	No	Yes	Yes
Wetland from FR	Yes	No	Yes	Yes	Yes
Wetland from WL	Yes	Yes	Yes	Yes	Yes
Monsoon - 2011–2012					
Wetland from BL	Yes	Yes	No	Yes	Yes
Wetland from AL	Yes	Yes	Yes	Yes	Yes
Wetland from RCS	No	No	No	Yes	Yes
Wetland from FR	Yes	No	Yes	Yes	Yes
Wetland from WL	Yes	Yes	Yes	Yes	Yes

BL: barren land; AL: agricultural land; RCS: rivers/canals/streams; FR: forest and WL: wasteland/gullied or riverine land.

Table 7
Wetland spectral separability for winter season generated using MODIS (1 km) data.

Wetland separability	Bands/indices				
	B2	B6	B19	NDVI	WMI
Winter - 2010–2011					
Wetland from BL	No	No	No	No	Yes
Wetland from AL	Yes	No	Yes	Yes	Yes
Wetland from RCS	No	No	No	No	Yes
Wetland from FR	No	No	No	Yes	Yes
Wetland from WL	No	No	No	Yes	Yes
Winter - 2011–2012					
Wetland from BL	No	No	No	Yes	Yes
Wetland from AL	Yes	No	Yes	Yes	Yes
Wetland from RCS	No	Yes	No	Yes	Yes
Wetland from FR	No	No	No	Yes	Yes
Wetland from WL	Yes	Yes	Yes	Yes	Yes

BL: barren land; AL: agricultural land; RCS: rivers/canals/streams; FR: forest and WL: wasteland/gullied or riverine land.

Table 8
Wetland spectral separability for summer season generated using MODIS (1 km) data.

Wetland separability	Bands/indices				
	B2	B6	B19	NDVI	WMI
Summer - 2010–2011					
Wetland from BL	No	No	No	No	No
Wetland from AL	Yes	Yes	Yes	Yes	Yes
Wetland from RCS	No	Yes	No	No	No
Wetland from FR	Yes	No	No	Yes	Yes
Wetland from WL	Yes	Yes	Yes	Yes	Yes
Summer - 2011–2012					
Wetland from BL	No	No	No	No	Yes
Wetland from AL	No	No	No	Yes	Yes
Wetland from RCS	No	No	No	No	Yes
Wetland from FR	No	No	No	Yes	Yes
Wetland from WL	No	Yes	No	No	Yes

BL: barren land; AL: agricultural land; RCS: rivers/canals/streams; FR: forest and WL: wasteland/gullied or riverine land.

from other land class types with respect to NDVI, WMI and 3 MODIS bands i.e., bands-2, 6, and 19. Separability analysis results opined that WMI was the most optimal input layer for classification of wetlands using coarse resolution MODIS (1 km) data.

4. Discussion

4.1. Best band/index selection for wetland areal extent extraction

Present study has brought out that WMI, an index developed by normalization of the spectral values of band 6 (SWIR) and band 4 (green), exhibits highest wetland separability factor of 0.93 (Table 9) and represent most optimal input layer for wetland delineation/classification. This is because WMI minimizes the reflectance of wetlands by using SWIR band 6 which is a strong water absorption band and the reflected radiance of wetlands is lower in band 6 than other classes. In addition, SWIR band 6 is also very sensitive to leaf water content and soil moisture (Wang et al., 2008) and can discriminate the wetlands from land cover types on the basis of variations in water content of wetland vegetation and soils.

On the contrary, water features including wetlands generally show high reflectance in visible region i.e., green band displayed high reflectance values for wetlands as compared to other classes. Consequently, WMI is able to separate wetlands from almost all the other remaining class types (BL, AL, RCS, FR and WL) considerably well in all seasons during both the years (except wetland from BL and wetland from RCS in summer 2010–2011). Thus, WMI can be significantly used for wetland mapping and classification in spatial domain for large areas using remotely sensed multispectral datasets.

Study has also revealed that NDVI, normalized calculation of band 2 (NIR) and band 1 (Red), ranked second after WMI in separability analysis as it has shown second highest wetland separability factor of 0.76 (Table 9). Though the discrimination between wetland versus BL and wetland versus RCS is not very good in NDVI, it does differentiates the wetlands from forest, agriculture and wasteland pixels remarkably well in all seasons (except wetland from WL in summer-2010–2011) during both the years due to its sensitivity to vegetation density in different land cover classes.

Individual MODIS bands including bands 2 (NIR) and 6 (SWIR) ranked 3rd following WMI and NDVI with wetland separability factors of 0.43 and 0.40 respectively. The suitability of bands 2 and 6 for wetland classification in the present study can be explained by the fact that the wetlands show low reflectance values than other remaining class types in NIR and SWIR regions. Thus, wetlands can be easily delineated in NIR and SWIR bands as water bodies appear in darker tone and display sharp contrast in NIR and SWIR bands. Further, MODIS band 19 has been discarded in separability analysis due its lowest wetland separability factor of 0.26. Finally, WMI, NDVI and MODIS bands viz., bands 2 (NIR) and 6 (SWIR) were selected for wetland area mapping in the present research work as these input layer were found to be most suitable input layers for wetland area computations for MODIS (1 km) datasets.

4.2. Wetland area mapping

Spatially, the spread or areal extent of wetlands mapped using MODIS (1 km) data in Uttar Pradesh was found to about 140,071 ha during 2010–2011 and 148,638 ha during 2011–2012 (Table 10). As it is known, MODIS (1 km) data is a coarse resolution data, there can be

Table 9
Wetland separability factor estimation for different MODIS (1 km) bands and indices.

Bands/indices	Total number of class combinations used for Separability analysis on 2010–2011 and 2011–2012 MODIS data	Total numbers of class combinations separated on 2010–2011 and 2011–2012 MODIS data	Wetland separability factor
WMI	30	28	28/30 = 0.93
NDVI	30	23	23/30 = 0.76
MODIS band 2	30	13	13/30 = 0.43
MODIS band 6	30	12	12/30 = 0.40

Table 10
MODIS (1 km) wetland area (ha) estimated for Uttar Pradesh.

Season	Sampling year			
	2010–2011		2011–2012	
	MODIS full pixel area	Sub-pixel/ actual MODIS area[b]	MODIS full pixel area	Sub-pixel/ actual MODIS area
Monsoon[a]	180,463	135,347	194,676	146,007
Winter	146,233	109,675	152,822	114,617
Summer	93,517	70,138	98,416	73,812
Net wetland area per year	140,071	105,053	148,638	111,479

[a] Due to the non-availability of MODIS data for monsoon season owing to cloud cover, MODIS data available for the month of October has been used to estimate wetland areas for monsoon season.
[b] Considering the paucity of AWiFS datasets, constant wetland area fraction of 0.75, estimated using AWiFS data for monsoon 2010, has been used throughout the study to estimate sub-pixel/actual wetland area for all the MODIS (1 km) datasets.

Table 11
Wetland area fraction (WAF) computed for the state of Uttar Pradesh using finer resolution AWiFS (56 m) data for Monsoon-2010.

Wetland feature	AWiFS wetland area (monsoon 2010)	AWiFS masked out wetland area outside the MODIS (1 km) class map (monsoon 2010)	WAF of total AWiFS wetland area
Open water	161,252 ha	81,484 ha	0.25
Aquatic vegetation	169,005 ha	164,846 ha	0.50
Total	330,257 ha	246,330 ha	0.75

spectral mixing of wetland pixels with other land cover types leading to significant errors in wetland area estimates. In view of this, wetland areas calculated using MODIS (1 km) data were further improved by using medium resolution Resourcesat-2 AWiFS (56 m) data to reduce discrepancy in wetland area estimates extracted using MODIS data. Wetland area estimated using MODIS (1 km) data was multiplied by WAF of 0.75 calculated from AWiFS (56 m) data to get the sub-pixel MODIS wetland area which represents actual wetland area (Tables 10 and 11) for each season/dataset in both the sampling years.

The actual MODIS wetland area for UP varied from 105,053 ha in 2010–2011 to 111,479 ha in 2011–2012 occupying approximately 0.44% (2010–2011)–0.46% (2011–2012) of the total geographical area of Uttar Pradesh, India. The accuracy of WAF estimated using AWiFS imagery with moderate resolution (56 m) can be improved by incorporating very high resolution datasets such as LANDSAT (Thematic Mapper/Enhanced Thematic Mapper Plus)/Google Earth Imagery to further refine the sub-pixel/actual MODIS wetland areal extent of UP.

Wetland mapping results also showed that temporally area under wetlands in monsoon season was higher as compared to winter and summer seasons (Table 10, Figs. 10 and 11) because of increased water spread due to monsoon rains. Many temporary wetlands which otherwise remain dry during summer, get flooded and lead to increment in wetland areal extent during monsoon season. In addition to this, some permanent wetlands that were too small to be detected in summer season probably became larger and detectable in monsoon (Roeck et al., 2008). On the contrary, summer season exhibited lowest wetland area which can be attributed to reduction in number and water surface area in wetlands due to disappearance of temporary wetlands and water recession in periphery of permanent wetlands. Thus, summer season imagery predominantly contains large/permanent wetlands which remain flooded throughout the year.

4.3. Classification accuracies for MODIS (1 km) datasets

Classification accuracy assessment (Tables 12 and 13) showed that summer season exhibited low overall classification accuracies of 87% in 2010–2011 and 85% in 2011–2012 with low values of Kappa coefficient (0.733 during 2010–2011 and 0.700 during 2011–2012). This was due to the mixed spectral signals received from shallow flooding water, exposed peripheral soils and aquatic vegetation leading to misclassification of periphery pixels in wetlands in summer. In contrast, monsoon season showed maximum overall accuracy of 92% with Kappa coefficient of 0.833 in both the years mainly because clear delineation of water from peripheral soil pixels/aquatic vegetation in monsoon due to enhanced water volume and surface area of wetlands.

5. Summary and concluding remarks

Extensive inter-band correlations and high data dimensionalities are the foremost tribulations associated with the multispectral data analysis such as MODIS data. Present investigation is an attempt to assess the importance and utility of coarse resolution multispectral MODIS (1 km) data in wetland delineation and mapping by developing an appropriate

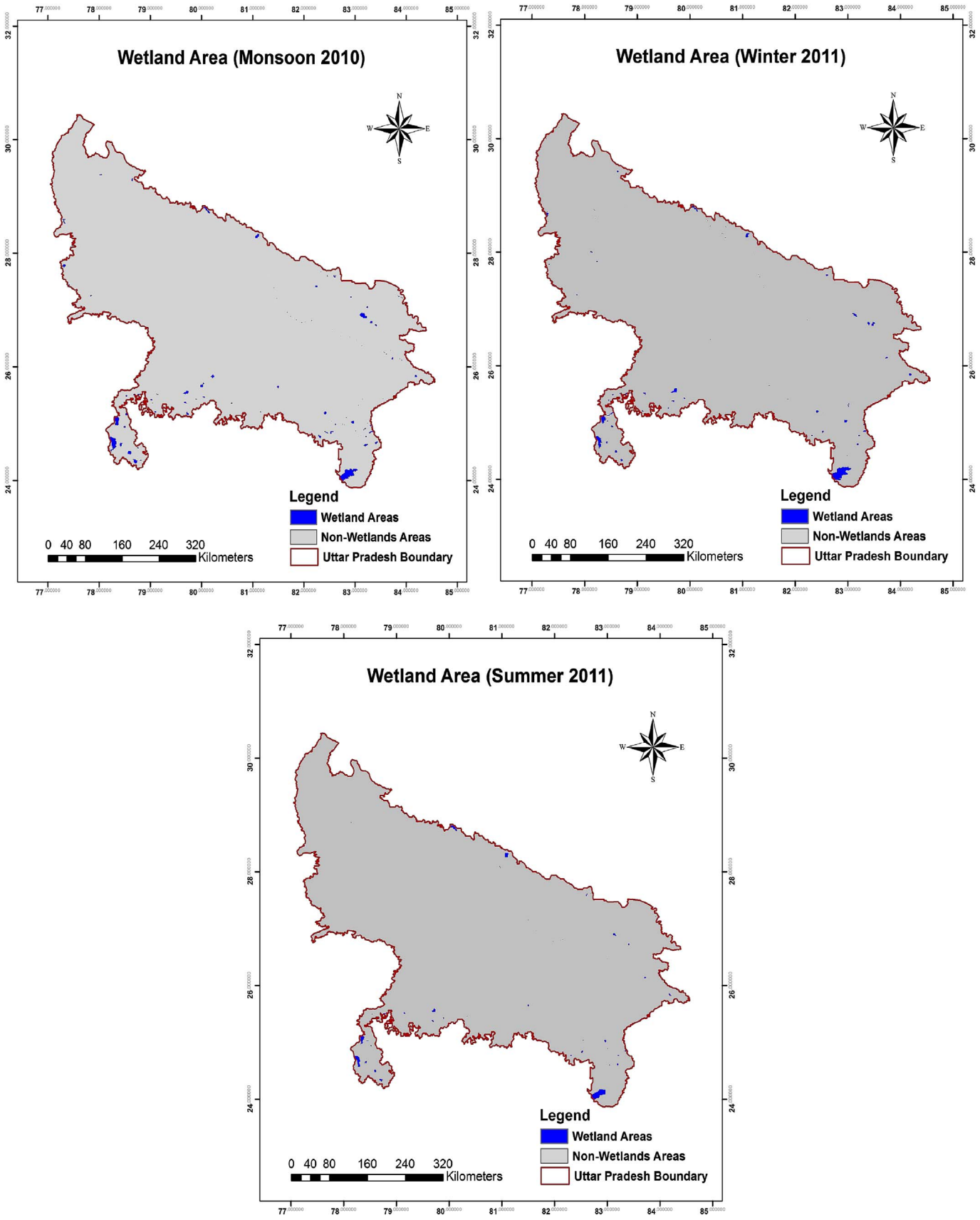

Fig. 10. Seasonal variations in wetland areal extent obtained during 2010–2011.

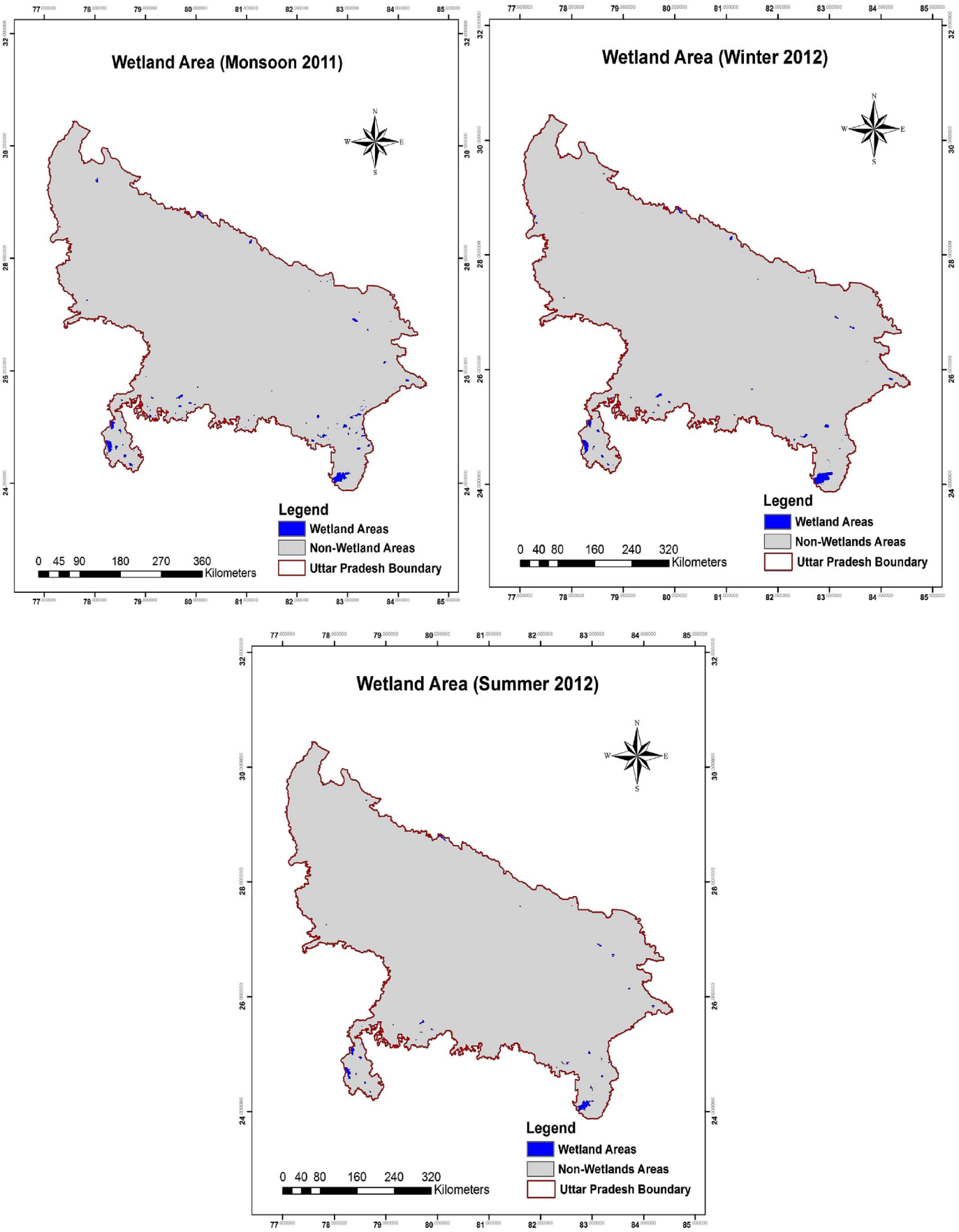

Fig. 11. Seasonal variations in wetland areal extent obtained during 2011–2012.

Table 12
Accuracy assessment for MODIS (1 km) data for 2010–2011.

Season	Land cover category	Producer accuracy (%)	User accuracy (%)
Monsoon 2010	Wetland areas	83.00	100.00
	Non-wetland areas	100.00	86.00
	Overall accuracy (%) = 92.00		
	Kappa coefficient = 0.833		
Monsoon 2011	Wetland areas	83.00	100.00
	Non-wetland areas	100.00	86.00
	Overall accuracy (%) = 92.00		
	Kappa coefficient = 0.833		
Winter 2011	Wetland areas	77.00	100.00
	Non-wetland areas	100.00	81.00
	Overall accuracy (%) = 88.00		
	Kappa coefficient = 0.767		

Table 13
Accuracy assessment for MODIS (1 km) data for 2011–2012.

Season	Land cover category	Producer accuracy (%)	User accuracy (%)
Winter 2012	Wetland areas	70.00	100.00
	Non-wetland areas	100.00	77.00
	Overall accuracy (%) = 85.00		
	Kappa coefficient = 0.700		
Summer 2011	Wetland areas	73.00	100.00
	Non-wetland areas	100.00	79.00
	Overall accuracy (%) = 86.67		
	Kappa coefficient = 0.733		
Summer 2012	Wetland areas	70.00	100.00
	Non-wetland areas	100.00	77.00
	Overall accuracy (%) = 85.00		
	Kappa coefficient = 0.700		

and suitable methodology. In the present work, a novel strategy based on the use of PCA, BTBC analysis, SDA and separability analysis has been evolved and applied to analyze the MODIS (1 km) data to capture the maximum and reliable information about wetlands by discarding the highly correlated bands and indices. Results of this integrated novel strategy used in present research work have amply proved that the dimensionality of MODIS data has been reduced from 24 input layers (22 optical MODIS bands, NDVI and WMI) to mere 4 input layers (WMI, NDVI, MODIS bands viz. NIR band 2 and SWIR band 6), thus reducing the volume of the dataset by approximately 83.33%. These extracted 4 input layers contain most of the important and useful information required for estimating wetland areal extent using multispectral MODIS (1 km) data. Wetland mapping results have shown that the magnitude of wetland areal extent estimated using MODIS data was about 140,071 ha during 2010–2011 and 148,638 ha during 2011–2012. Further, AWiFS imagery with moderate resolution (56 m) was used to improve the MODIS wetland area estimates and sub-pixel/actual MODIS wetland areal extent for the state of UP varied from 105,053 ha in 2010–2011 to 111,479 ha in 2011–2012.

Another vital aspect of this work is the newly developed WMI (Wetland Model Index) which represents the most optimal input layer to discriminate wetlands from built-up land, agricultural land, rivers/canals/streams, forest and wasteland with maximum wetland separability factor of 0.93. Thus, this study pioneers in proposing and justifying the utility of WMI in future studies related to wetland mapping and classification. Conclusively, combined with medium resolution data and analyzed through well integrated approach, MODIS (1 km) data, though having high data dimensionality and spectral mixing, can be successfully utilized to map and monitor the wetlands over large areas, especially for research requiring high spatial and temporal resolutions.

Acknowledgements

The authors wish to thank Dr. Anshu Miglani, Assistant Director, IGNOU, Delhi and Dr. Reshu Aggarwal for their kind support and assistance in MODIS data analysis.

Appendix A

Table A1
22 MODIS optical bands used for analysis.

Layer no.	Layer name	Wavelength (μm)	Resolution (m)	General applicability
1	MODIS B1	0.620–0.670 (red)	250	Land/cloud/aerosol boundaries
2	MODIS B2	0.841–0.876 (NIR)	250	
3	MODIS B3	0.459–0.479 (blue)	500	Land/cloud/aerosol properties
4	MODIS B4	0.545–0.565 (green)	500	
5	MODIS B5	1.23–1.25 (NIR)	500	
6	MODIS B6	1.628–1.652 (SWIR)	500	
7	MODIS B7	2.105–2.155 (SWIR)	500	
8	MODIS B8	0.405–0.42 (blue)	1000	Ocean colour/phytoplankton/biogeochemistry
9	MODIS B9	0.438–0.448 (blue)	1000	
10	MODIS B10	0.483–0.493 (blue)	1000	
11	MODIS B11	0.526–0.536 (green)	1000	
12	MODIS B12	0.546–0.556 (green)	1000	
33	MODIS B13	0.662–0.672 (red)	1000	
14	MODIS B14	0.673–0.683 (red)	1000	
15	MODIS B15	0.743–0.753 (red)	1000	
16	MODIS B16	0.862–0.877 (NIR)	1000	
17	MODIS B17	0.89–0.92 (NIR)	1000	Atmospheric water vapour surface/cloud temperature
18	MODIS B18	0.931–0.941 (NIR)	1000	
19	MODIS B19	0.915–0.965 (NIR)	1000	
20	MODIS B20	3.66–3.84 (MWIR)	1000	
21	MODIS B21	3.929–3.989 (MWIR)	1000	
22	MODIS B22	3.929–3.989 (MWIR)	1000	

Table A2
Major specifications of AWiFS.
Source: http://www.nrsc.gov.in/data_rs2/Resourcesat-2_Handbook.pdf.

Orbit	Circular, sun-synchronous near polar orbit with an inclination of 98.69°, at an altitude of 817 km
Equatorial crossing time	10:30 AM ± 10 min (at descending mode)
Data rate	105 Mbps
Spatial resolution	56 m at nadir and 70 m at field edges
Quantization	12 bits
Temporal resolution	5 days
Swath	740 km
Spectral bands	B2: 0.52–0.59 μm
	B3: 0.62–0.68 μm
	B4: 0.77–0.86 μm
	B5: 1.55–1.70 μm

Table A3
Details of AWiFS data used for analysis.
Source: bhuvan.nrsc.gov.in/data/download/index.php.

S. no.	Date of acquisition	Toposheet number
1	3rd October 2010	g43e; g43f; h43e; h43k; h43l; h43q; h43r; h43w
2	28th October 2010	f43f; f44a; g43l; g43r; g43x; g44a; g44b; g44g; g44h; g44m; g44n; g44u; h43x; h44g; h44m; h44n; h44s; h44t; g44c; g44i; g44o; g44p; g44v; h44o; h44u; h44v; g44k; g44q; g44w; g44d; g44e; g44j
3	29th October 2010	f44e; g44f; g44l; g44r; g45a; g45g; g45h; g45m; g45n; g45t; f44f
4	2nd November 2010	g44s; g44t
5	27th November 2010	g44x; g45s

Table A4
List of abbreviations.

Abbreviation	Explanation
AL	agricultural land
AWiFS	Advanced Wide Field Sensor
BL	barren land
BTBC	Band to Band Correlation
EMS	electromagnetic spectrum
EOS	Earth Observation System
FOC	frequency of occurrence
FR	forest
GIS	Geographic Information System
IAF-HRI	Irrigated Area Fraction-High Resolution Imagery
LULC	land use-land cover
MIR	middle infra red
MODIS	Moderate Resolution Imaging Spectro-radiometer
NASA	National Aeronautics and Space Administration
NDVI	Normalized Difference Vegetation Index
NIR	near infra red
NRSC	National Remote Sensing Centre
PC	principal component
PCA	Principal Component Analysis
RCS	rivers/canals/streams
ROI	region of interest
RS	remote sensing
SAC	Space Applications Centre
SDA	Stepwise Discriminant Analysis
SWIR	short wavelength infra red
UP	Uttar Pradesh
WAF	wetland area fraction
WAF-FRI	Wetland Area Fraction-Finer Resolution Imagery
WL	wasteland/gullied or riverine land
WMI	Wetland Model Index

Table A5
Band to Band Correlation (BTBC) analysis for monsoon season.

S. no.	Input bands pairs selected for monsoon season					
	2010–2011			2011–2012		
	Band pairs		R^2	Band pairs		R^2
1	Band 5	Band 22	0.0046	Band 15	Band 22	0.0008
2	Band 22	Band 5	0.0046	Band 22	Band 15	0.0008
3	Band 2	Band 22	0.0085	Band 13	Band 22	0.0903
4	Band 18	Band 22	0.0097	Band 7	Band 22	0.1333
5	Band 17	Band 22	0.0099	Band 1	Band 22	0.2089
6	Band 16	Band 22	0.0109	Band 6	Band 22	0.2508
7	Band 14	Band 22	0.0121	Band 18	Band 15	0.2562
8	Band 19	Band 22	0.0128	Band 17	Band 15	0.2587
9	Band 6	Band 22	0.0246	Band 2	Band 15	0.2628
10	Band 21	Band 22	0.0259	Band 19	Band 15	0.2650
11	Band 8	Band 22	0.0261	Band 16	Band 15	0.2674
12	Band 9	Band 22	0.0295	Band 21	Band 15	0.2717
13	Band 12	Band 22	0.0305	Band 20	Band 15	0.2724
14	Band 3	Band 22	0.0315	Band 14	Band 15	0.2778
15	Band 11	Band 22	0.0323	Band 12	Band 22	0.2809
16	Band 4	Band 22	0.0326	Band 4	Band 22	0.2847
17	Band 10	Band 22	0.0337	Band 11	Band 22	0.2891
18	Band 13	Band 22	0.0416	Band 10	Band 22	0.2976
19	Band 20	Band 22	0.0419	Band 8	Band 15	0.3004
20	Band 1	Band 22	0.0453	Band 5	Band 15	0.3087
21	Band 7	Band 22	0.0546	Band 3	Band 22	0.3092
22	Band 15	Band 22	0.1070	Band 9	Band 22	0.3158

Table A6
Band to Band Correlation (BTBC) analysis for winter season.

S. no.	Input bands pairs selected for winter season					
	2010–2011			2011–2012		
	Band pairs		R^2	Band pairs		R^2
1	Band 21	Band 15	0.00005	Band 15	Band 20	0.00000
2	Band 15	Band 19	0.00006	Band 20	Band 15	0.00000
3	Band 19	Band 15	0.00006	Band 17	Band 15	0.00014
4	Band 2	Band 15	0.00028	Band 19	Band 15	0.00043
5	Band 20	Band 15	0.00057	Band 2	Band 15	0.00076
6	Band 22	Band 15	0.00216	Band 22	Band 15	0.00590
7	Band 18	Band 15	0.00650	Band 5	Band 15	0.00942
8	Band 17	Band 15	0.00650	Band 18	Band 15	0.01287
9	Band 5	Band 15	0.00728	Band 17	Band 15	0.01397
10	Band 16	Band 15	0.01352	Band 16	Band 15	0.01499
11	Band 8	Band 15	0.01402	Band 14	Band 15	0.01697
12	Band 13	Band 20	0.01584	Band 8	Band 15	0.02752
13	Band 9	Band 15	0.02091	Band 9	Band 15	0.03594
14	Band 12	Band 15	0.02427	Band 12	Band 15	0.03782
15	Band 3	Band 15	0.02642	Band 3	Band 15	0.04210
16	Band 9	Band 15	0.02909	Band 11	Band 15	0.04295
17	Band 14	Band 15	0.02980	Band 4	Band 15	0.04363
18	Band 4	Band 15	0.03075	Band 10	Band 15	0.04631
19	Band 10	Band 15	0.03078	Band 6	Band 15	0.04903
20	Band 6	Band 15	0.04927	Band 1	Band 15	0.08416
21	Band 1	Band 15	0.07956	Band 13	Band 20	0.11116
22	Band 7	Band 15	0.12841	Band 7	Band 15	0.11341

Table A7
Band to Band Correlation (BTBC) analysis for summer season.

S. no.	Input bands pairs selected for summer season					
	2010–2011			2011–2012		
	Band pairs		R^2	Band pairs		R^2
1	Band 5	Band 11	0.00001	Band 12	Band 22	0.282967
2	Band 11	Band 5	0.00001	Band 22	Band 12	0.282967
3	Band 3	Band 11	0.00002	Band 11	Band 22	0.457368
4	Band 21	Band 11	0.00003	Band 10	Band 22	0.483331
5	Band 19	Band 11	0.00004	Band 3	Band 22	0.485165
6	Band 9	Band 11	0.00010	Band 9	Band 22	0.487189
7	Band 10	Band 11	0.00018	Band 5	Band 22	0.493560
8	Band 20	Band 11	0.00030	Band 18	Band 22	0.495558
9	Band 8	Band 11	0.00086	Band 17	Band 22	0.495639
10	Band 6	Band 11	0.00090	Band 16	Band 22	0.495653
11	Band 4	Band 11	0.00159	Band 14	Band 22	0.495654
12	Band 15	Band 11	0.00344	Band 8	Band 22	0.495710
13	Band 13	Band 11	0.00386	Band 15	Band 22	0.496833
14	Band 18	Band 11	0.00391	Band 13	Band 22	0.497733
15	Band 17	Band 11	0.00392	Band 4	Band 22	0.498814
16	Band 14	Band 11	0.00392	Band 2	Band 22	0.502111
17	Band 16	Band 11	0.00392	Band 19	Band 22	0.510190
18	Band 7	Band 11	0.00480	Band 1	Band 22	0.510452
19	Band 1	Band 11	0.00526	Band 6	Band 22	0.519339
20	Band 2	Band 22	0.00774	Band 21	Band 22	0.525576
21	Band 22	Band 10	0.00815	Band 7	Band 22	0.533046
22	Band 12	Band 22	0.04163	Band 20	Band 22	0.535581

Table A8
Seasonal Wilk's Lambda and F values for monsoon season.

Wilk's Lambda and F values for monsoon season											
2010–2011						2011–2012					
Input waveband	Wilk's Lambda	F value	df1	df2	Sig.	Input waveband	Wilk's Lambda	F value	df1	df2	Sig.
Band 2	0.204	3506.071	5	4498	0.000	Band 5	0.277	2560.691	5	4895	0.000
Band 19	0.215	3288.000	5	4498	0.000	Band 19	0.279	2531.492	5	4895	0.000
Band 21	0.268	2453.402	5	4498	0.000	Band 2	0.281	2503.473	5	4895	0.000
Band 5	0.282	2286.201	5	4498	0.000	Band 21	0.306	2221.645	5	4895	0.000
Band 6	0.354	1641.243	5	4498	0.000	Band 6	0.342	1882.042	5	4895	0.000
Band 1	0.355	1635.685	5	4498	0.000	Band 20	0.371	1657.853	5	4895	0.000
Band 20	0.359	1604.121	5	4498	0.000	Band 18	0.415	1379.266	5	4895	0.000
Band 11	0.401	1342.412	5	4498	0.000	Band 10	0.456	1167.403	5	4895	0.000
Band 15	0.432	1182.812	5	4498	0.000	Band 13	0.469	1109.091	5	4895	0.000
Band 4	0.436	1165.159	5	4498	0.000	Band 7	0.470	1103.222	5	4895	0.000
Band 10	0.440	1144.224	5	4498	0.000	Band 3	0.482	1054.072	5	4895	0.000
Band 13	0.445	1122.281	5	4498	0.000	Band 11	0.490	1017.491	5	4895	0.000
Band 7	0.447	1111.210	5	4498	0.000	Band 15	0.533	857.920	5	4895	0.000
Band 18	0.452	1090.311	5	4498	0.000	Band 9	0.540	834.176	5	4895	0.000
Band 3	0.493	924.349	5	4498	0.000	Band 14	0.552	795.522	5	4895	0.000
Band 17	0.548	741.199	5	4498	0.000	Band 4	0.557	779.700	5	4895	0.000
Band 9	0.595	611.446	5	4498	0.000	Band 1	0.578	714.788	5	4895	0.000
Band 8	0.706	375.434	5	4498	0.000	Band 8	0.623	591.975	5	4895	0.000
Band 22	0.794	232.794	5	4498	0.000	Band 17	0.642	545.729	5	4895	0.000
Band 14	0.800	225.530	5	4498	0.000	Band 22	0.687	446.579	5	4895	0.000
Band 16	0.950	47.515	5	4498	0.000	Band 12	0.758	312.743	5	4895	0.000
Band 12	0.959	38.024	5	4498	0.000	Band 16	0.799	245.529	5	4895	0.000

Table A9
Seasonal Wilk's Lambda and F values for winter season.

Wilk's Lambda and F values for winter season											
2010–2011						2011–2012					
Input waveband	Wilk's Lambda	F value	df1	df2	Sig.	Input waveband	Wilk's Lambda	F value	df1	df2	Sig.
Band 13	0.252	2064.3	5	3486	0.00	Band 20	0.258	2078.6	5	3605	0.000
Band 15	0.280	1797.0	5	3486	0.00	Band 21	0.258	2071.3	5	3605	0.000
Band 4	0.304	1597.2	5	3486	0.00	Band 19	0.276	1888.1	5	3605	0.000
Band 11	0.319	1485.2	5	3486	0.00	Band 2	0.290	1763.1	5	3605	0.000
Band 1	0.325	1448.2	5	3486	0.00	Band 15	0.328	1474.4	5	3605	0.000
Band 20	0.357	1253.2	5	3486	0.00	Band 7	0.356	1304.3	5	3605	0.000
Band 21	0.361	1233.1	5	3486	0.00	Band 1	0.378	1187.7	5	3605	0.000
Band 19	0.383	1123.7	5	3486	0.00	Band 6	0.466	826.2	5	3605	0.000
Band 10	0.394	1070.6	5	3486	0.00	Band 5	0.477	789.7	5	3605	0.000
Band 2	0.398	1053.6	5	3486	0.00	Band 4	0.525	652.2	5	3605	0.000
Band 8	0.404	1027.2	5	3486	0.00	Band 22	0.530	640.3	5	3605	0.000
Band 7	0.410	1001.4	5	3486	0.00	Band 18	0.552	585.9	5	3605	0.000
Band 3	0.478	760.9	5	3486	0.00	Band 11	0.553	581.9	5	3605	0.000
Band 9	0.499	699.2	5	3486	0.00	Band 13	0.594	492.6	5	3605	0.000
Band 22	0.596	473.5	5	3486	0.00	Band 10	0.631	422.1	5	3605	0.000
Band 6	0.630	409.7	5	3486	0.00	Band 8	0.686	330.3	5	3605	0.000
Band 18	0.682	324.7	5	3486	0.00	Band 3	0.687	329.1	5	3605	0.000
Band 17	0.686	319.2	5	3486	0.00	Band 9	0.688	327.2	5	3605	0.000
Band 5	0.696	304.6	5	3486	0.00	Band 17	0.706	300.5	5	3605	0.000
Band 12	0.767	211.9	5	3486	0.00	Band 16	0.932	52.3	5	3605	0.000
Band 14	0.806	167.6	5	3486	0.00	Band 14	0.935	50.2	5	3605	0.000
Band 16	0.816	157.4	5	3486	0.00	Band 12	0.945	42.2	5	3605	0.000

Table A10
Seasonal Wilk's Lambda and F values for summer season.

Wilk's Lambda and F values for summer season											
2010–2011						2011–2012					
Input waveband	Wilk's Lambda	F value	df1	df2	Sig.	Input waveband	Wilk's Lambda	F value	df1	df2	Sig.
Band 4	0.322	1558.803	5	3703	0.000	Band 4	0.4376	964.509	5	3752	0.000
Band 10	0.356	1337.974	5	3703	0.000	Band 1	0.4422	946.523	5	3752	0.000
Band 3	0.366	1282.768	5	3703	0.000	Band 3	0.4977	757.405	5	3752	0.000
Band 9	0.403	1097.438	5	3703	0.000	Band 9	0.5048	736.027	5	3752	0.000
Band 1	0.442	934.932	5	3703	0.000	Band 7	0.5114	716.898	5	3752	0.000
Band 5	0.454	890.320	5	3703	0.000	Band 6	0.5240	681.671	5	3752	0.000
Band 8	0.466	848.541	5	3703	0.000	Band 2	0.5281	670.601	5	3752	0.000
Band 2	0.473	826.341	5	3703	0.000	Band 19	0.5477	619.680	5	3752	0.000
Band 19	0.488	775.568	5	3703	0.000	Band 5	0.5478	619.388	5	3752	0.000
Band 11	0.517	691.066	5	3703	0.000	Band 8	0.5809	541.491	5	3752	0.000
Band 12	0.552	601.845	5	3703	0.000	Band 21	0.5940	512.942	5	3752	0.000
Band 6	0.581	535.052	5	3703	0.000	Band 20	0.6547	395.840	5	3752	0.000
Band 21	0.591	512.977	5	3703	0.000	Band 12	0.7068	311.295	5	3752	0.000
Band 7	0.597	500.495	5	3703	0.000	Band 15	0.8399	142.997	5	3752	0.000
Band 20	0.749	248.626	5	3703	0.000	Band 13	0.8694	112.734	5	3752	0.000
Band 15	0.782	207.011	5	3703	0.000	Band 11	0.8697	112.380	5	3752	0.000
Band 22	0.803	181.152	5	3703	0.000	Band 10	0.9162	68.679	5	3752	0.000
Band 18	0.862	118.738	5	3703	0.000	Band 18	0.9198	65.465	5	3752	0.000
Band 17	0.949	39.401	5	3703	0.000	Band 17	0.9468	42.167	5	3752	0.000
Band 13	0.968	24.767	5	3703	0.000	Band 22	0.9755	18.819	5	3752	0.000
Band 14	.(a)					Band 14	0.9980	1.468	5	3752	0.197
Band 16	.(a)					Band 16	0.9980	1.468	5	3752	0.197

.(a) = cannot be computed because this variable is a constant.

References

Alphan, H., Yilmaz, K., 2005. Monitoring environmental changes in the Mediterranean coastal landscape: the case of Cukurova, Turkey. Environ. Manag. 35, 607–619.

Chakraborty, K., 2009. Vegetation change detection in Barak Basin. Curr. Sci. 96, 1236–1241.

Chen, L., Jin, Z., Michishita, R., Cai, J., Yue, T., Chen, B., Xu, B., 2014. Dynamic monitoring of wetland cover changes using time-series remote sensing imagery. Eco. Inform. 24, 17–26.

Dong, Z., Wang, Z., Liu, D., Song, K., Li, L., Jia, M., Ding, Z., 2014. Mapping wetland areas using Landsat-derived NDVI and LSWI: a case study of West Songnen Plain, Northeast China. J. Indian Soc. Remote Sens. 42, 569–576.

Fung, T., Ledrew, E., 1987. Application of principal component analysis to change detection. Photogramm. Eng. Remote. Sens. 53, 1649–1658.

Galvao, L.S., Formaggio, A.R., Tisot, D.A., 2005. Discrimination of sugarcane varieties in southeastern Brazil with EO-1 hyperion data. Remote Sens. Environ. 95, 23–534.

Garg, J.K., 2015. Wetland assessment, monitoring and management in India using geospatial techniques. J. Environ. Manag. 148, 112–123.

Garg, J.K., Singh, T.S., Murthy, T.V.R., 1998. Wetlands of India. In: Project Report: RSAM/SAC/RESA/PR/01/98. Space Applications Centre (ISRO), Ahmedabad, India (239 pp.).

Hillger, D.W., Clark, J.D., 2002. Principal component image analysis of MODIS for volcanic ash. Part I: most important bands and implications for future GOES imagers. J. Appl. Meteorol. 41, 985–1001.

Jensen, J.R., 1996. Introductory Digital Image Processing: A Remote Sensing Perspective, 2nd ed. Prentice Hall, Upper Saddle River, New Jersey (316 pp.).

Jha, S.N., 2007. Uttar Pradesh: The Land and the People. National Book Trust, India.

Joseph, G., 2005. Fundamentals of Remote Sensing, Second edition. University Press, Hydrabad.

Liang, S., 2004. Quantitative Remote Sensing of Land Surfaces. John Wiley & Sons, New Jersey, pp. 246–268.

Miettinen, J., 2007. Variability of fire–induced changes in MODIS surface reflectance by land - cover type in Borneo. Int. J. Remote Sens. 28, 4967–4984.

Miglani, A., 2009. Study on the Utility of Satellite and Ground Based Hyperspectral Remote Sensing Data for the Retrieval of Crop Biophysical Parameters. (PhD thesis) Hemwati Nandan Bahuguna Garhwal University, India.

Miglani, A., Ray, S.S., Pandey, R., Parihar, J.S., 2008. Evaluation of EO-1 hyperion data for agricultural applications. J. Indian Soc. Remote Sens. 36, 255–266.

Ray, S.S., Jain, N., Das, G., Miglani, A., Panigrahy, S., Parihar, J.S., Singh, J.P., Singh, A.K., Rachna, 2007. Use of hyperspectral remote sensing in agricultural applications: ground-based studies. In: Project Report: SAC/RESA/AFEG/PF/SN/07/2007. Space Applications Centre (ISRO), Ahmedabad, India.

Roeck, E.R.D., Verhoest, N.E.C., Miya, M.H., Lievens, H., Batelaan, O., Thomas, A., Brendonck, L., 2008. Remote sensing and wetland ecology: a South African case study. Sensors 8, 3542–3556.

Rouse Jr., J.W., Haas, R.H., Schell, J.A., Deering, D.W., 1973. Monitoring vegetation systems in the Great Plains with ERTS. In: Freden, S.C., Mercanti, E.P., Becker, M. (Eds.), Third Earth Resources Technology Satellite-1 Symposium. Technical Presentations, Section A, Vol. I. National Aeronautics and Space Administration (NASA SP-351), Washington, DC, pp. 309–317.

SAC, 2011. National Wetland Atlas. Space Application Centre (ISRO), Ahmedabad, India.

Singh, A., Harrison, A., 1985. Standardized principal components. Int. J. Remote Sens. 6, 883–896.

Thenkabail, P.S., 2002. Optimal hyperspectral narrowbands for discriminating agricultural crops. Remote Sens. Rev. 20, 257–291.

Thenkabail, P.S., Enclona, E.A., Ashton, M.S., Meer, B.V.D., 2004. Accuracy assessments of hyperspectral waveband performance for vegetation analysis applications. Remote Sens. Environ. 91, 354–376.

Thenkabail, P.S., Biradar, C.M., Noojipady, P., Cai, X., Dheeravath, V., Li, Y., Velpuri, M., Gumma, M., Pandey, S., 2007. Sub-pixal area calculation methods for estimating irrigated areas. Sensors 7, 2519–2538.

Wang, L., Qu, J.J., Hao, X., Zhu, Q., 2008. Sensitivity studies of the moisture effects on MODIS SWIR reflectance and vegetation water indices. Int. J. Remote Sens. 29, 7065–7075.